Nowe kierunki badań struktury nukleonu

Andrzej Sandacz

Instytut Problemów Jądrowych, Warszawa

Seminarium Fizyki Wielkich Energii, Uniwersytet Warszawski

12 stycznia 2007

Kierunki tradycyjne

- Rozkłady partonów

rozkłady prawdopodonieństw, niezależne od spinu bądź zależne od skrętności dla kwarków o różnych zapachach i dla gluonów

dostępne w: DIS, SIDIS, DY, ‘twardych’ oddziaływaniach pp/ppbar, …

dla ustalonej ‘twardości’ oddziaływania, zależą tylko od 1 zmiennej: ułamka pedu nukleonu niesionego przez parton (x_{Bj})

- Formfaktory nukleonów

elektryczne, magnetyczne, aksjalne, dziwności, …

zależą tylko od 1 zmiennej: kwadratu przekazu czteropędu (t)

w reprezentacji położeniowej odpowiadają rozkładom prawdopodobieństw w płaszczyźnie prostopadłej do osi zderzenia

Nowe kierunki

- Uogólnione rozkłady partonów (GPDs)

  badane w **'twardych' procesach ekskluzywnych**

  np. $e\,p \longrightarrow e\,p\,\gamma$ (DVCS)

- Zależne od pędu poprzecznego (TMD) rozkłady partonów i funkcje fragmentacji

  badane poprzez asymetrie rozkładów azymutalnych w **'twardych' procesach SIDIS**

  np. $e\,p^{\uparrow} \longrightarrow e\,\pi^{+}X$ ==> m.in. **Collins** and **Sievers** effects

- Rozkłady poprzecznego spinu kwarków (transversity)

  analog tradycyjnych rozkładów partonów, ale dla spinu poprzecznego

  obecnie badane w **'twardych' procesach SIDIS**

Konferencje dot. GPDs and TMDs w 2006

Trento, Italy June 5 - 9, 2006

Villa Mondragone, Monte Porzio Catone
Rome, Italy June 12 - 16, 2006

Hard Exclusive Processes at JLab 12 GeV and a Future EIC

University of Maryland College Park
October 29 - 30, 2006

Plan referatu

- Wprowadzenie
- Modelowanie GPDs i obliczenia na sieci QCD
- Orbitalny moment pędu kwarków
- Dane doświadczalne dla DVCS
- Tomografia hadronów
- Efekt Sieversa
- Planowane doświadczenia

PDs and GPDs

$e\,p \rightarrow e\,X$

$e\,p \rightarrow e\,p\,\gamma$

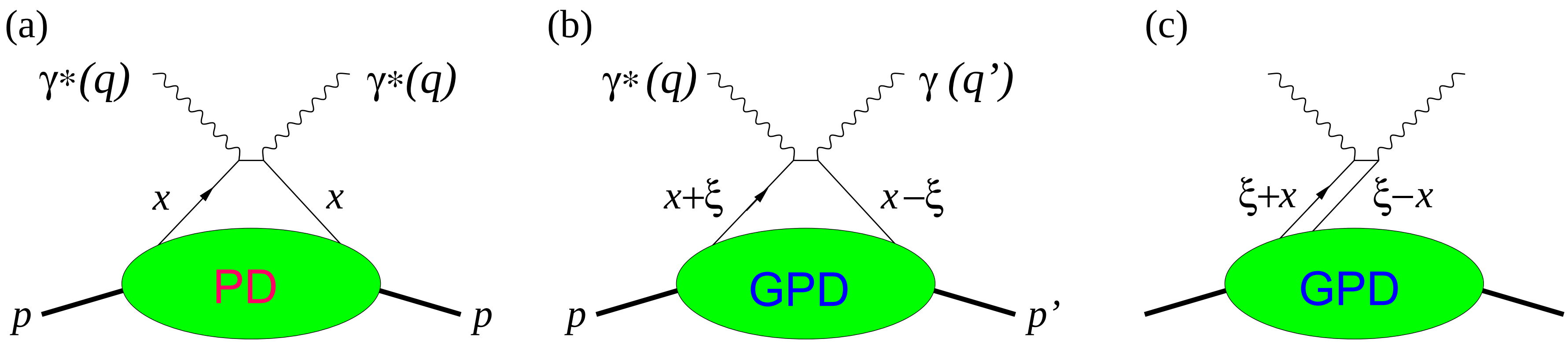

$\sigma(\gamma^{*}p \rightarrow X) \sim$
$\mathrm{Im}\, A(\gamma^{*}p \rightarrow \gamma^{*}p)_{t=0}$ ⟷ $\sigma(\gamma^{*}p \rightarrow \gamma\, p) \sim |\, A(\gamma^{*}p \rightarrow \gamma\, p)\, |^{2}$

for given Q^2 depends only on x_B $(\equiv x)$ ⟷ $A(\xi\,, t)$

$\xi \approx x_B / (2 - x_B)$, $x_B = Q^2/(2pq)$

Generalized Parton Distributions

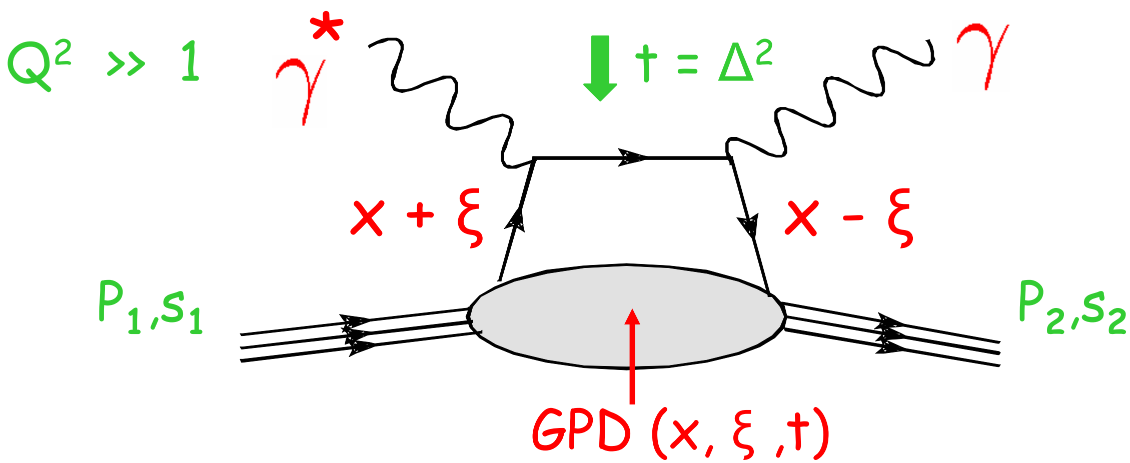

low -t process :
-t << Q^2

We use the notation of X.Ji and name the momenta according to:

$$h(P_1) + \Gamma^*(q_1) \rightarrow h(P_2) + \Gamma(q_2)$$

with $\Delta_\mu = q_{2\mu} - q_{1\mu}$, $t = \Delta^2$, $P_\mu = (P_{1\mu} + P_{2\mu})/2$ and $\xi = -Q^2/2P \cdot q$.

$$\int \frac{dz^-}{2\pi} e^{ixP^+z^-} \langle P_2 | \, \bar{q}(-\frac{1}{2}z) \, \gamma^+ q(\frac{1}{2}z) \, | P_1 \rangle \Big|_{z^+=0, z_\perp=0}$$

$$= \frac{1}{P+} \left[H_q(x,\xi,t) \, \bar{N}(P_2)\gamma^+ N(P_1) + E_q(x,\xi,t) \, \bar{N}(P_2) \frac{i\sigma^{+\alpha}\Delta_\alpha}{2M} N(P_1) \right]$$

$$\int \frac{dz^-}{2\pi} e^{ixP^+z^-} \langle p' | \, \bar{q}(-\frac{1}{2}z) \, \gamma^+ \gamma_5 \, q(\frac{1}{2}z) \, | p \rangle \Big|_{z^+=0, z_\perp=0}$$

$$= \frac{1}{P+} \left[\tilde{H}_q(x,\xi,t) \, \bar{N}(P_2)\gamma^+ \gamma_5 N(P_1) + \tilde{E}_q(x,\xi,t) \, \bar{N}(P_2) \frac{\gamma_5 \Delta^+}{2M} N(P_1) \right]$$

Properties of GPDs

various parton processes embodied in a given single GPD

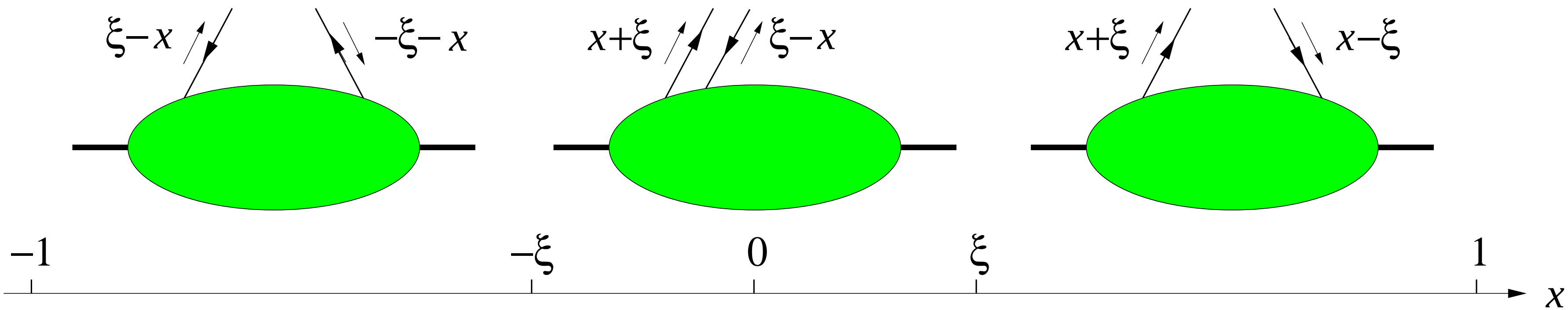

$x < -\xi$ — $\bar{q}$ **out** $\bar{q}$ **in**

$-\xi < x < \xi$ — $q\bar{q}$ **out**

$x > \xi$ — q **out** q **in**

Properties of GPDs

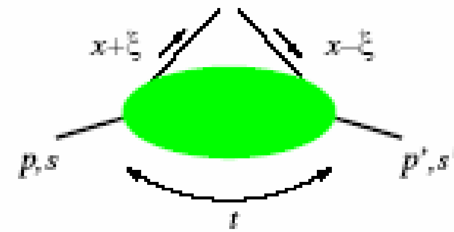

$H^q, \widetilde{H}^q \leftrightarrow s = s'$ for $p = p'$ recover usual parton densities

$$H^q(x,0,0) = q(x), \quad \widetilde{H}^q(x,0,0) = \Delta q(x) \quad for\ x > 0$$
$$H^q(x,0,0) = -q(-x), \quad \widetilde{H}^q(x,0,0) = \Delta q(-x) \quad for\ x < 0$$

$E^q, \widetilde{E}^q \leftrightarrow s \neq s'$ decouples for $p = p'$

$E^q, \widetilde{E}^q \neq 0$ **needs** orbital angular momentum between partons

$$\int dx\, H^q(x,\xi,t) = F_1^q(t) \quad \textbf{Dirac}$$
$$\int dx\, E^q(x,\xi,t) = F_2^q(t) \quad \textbf{Pauli}$$
$$\int dx\, \widetilde{H}^q(x,\xi,t) = g_A^q(t) \quad \textbf{axial}$$
$$\int dx\, \widetilde{E}^q(x,\xi,t) = g_P^q(t) \quad \textbf{pseudoscalar}$$

Ji's sum rule $\frac{1}{2}\int dx\, x\,(H^q + E^q) = J^q(t)$

$J^q(0)$ **total** angular momentum carried by quark flavour *q* (helicity and **orbital** part)

Observables and their relationship to GPDs

$$T^{DVCS} = \int_{-1}^{+1} \frac{GPD(x,\xi,t)}{x-\xi+i\varepsilon}\,dx \quad + \quad \cdots$$

$$= P\int_{-1}^{+1} \frac{GPD(x,\xi,t)}{x-\xi}\,dx \quad - \quad i\pi\, GPD(x=\xi,\xi,t) \quad + \quad \cdots$$

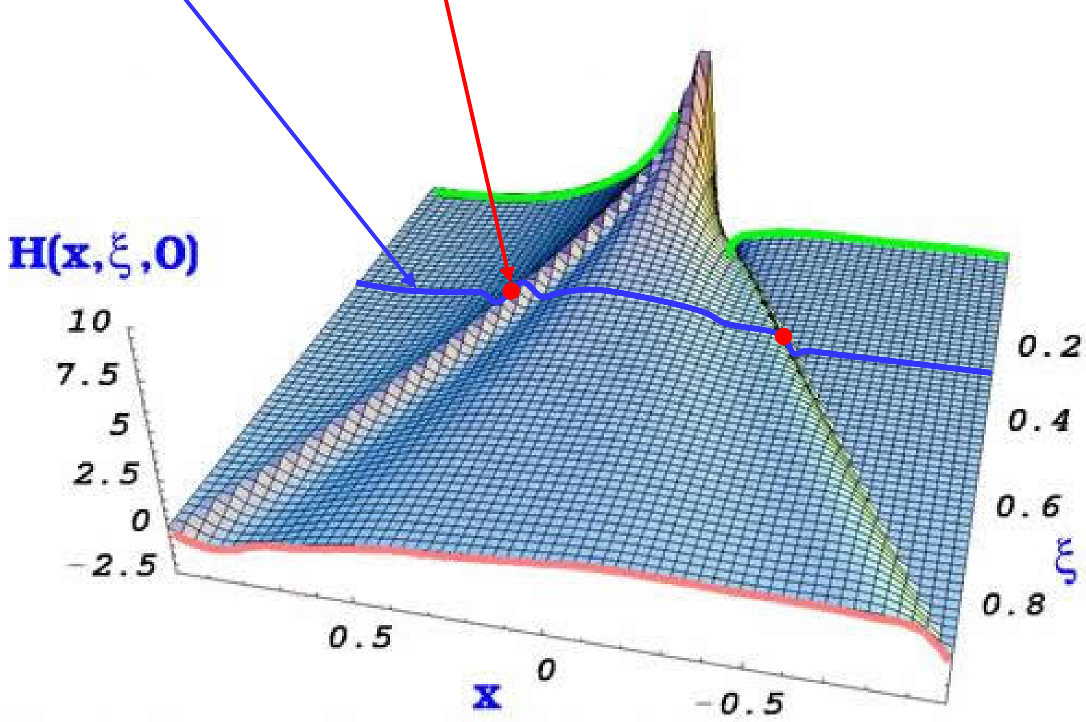

Shorthand notation:

$$T^{DVCS} = \{\mathcal{H}, \widetilde{\mathcal{H}}, \mathcal{E}, \widetilde{\mathcal{E}}\}$$

$$GPD = \{H, \widetilde{H}, E, \widetilde{E}\}$$

Other processes related to GPDs

- exclusive meson production

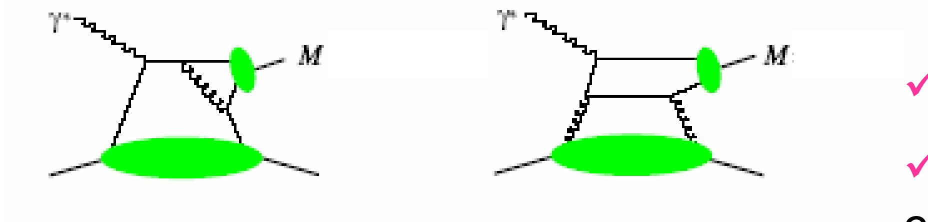

$M = \rho, \pi, \varphi, J/\psi, \ldots$

✓ meson distribution amplitude (DA) appears

✓ access to different spin and flavour combinations of GPDs of quarks and gluons

- 2 π production

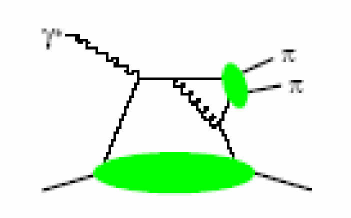

similar to EMP

- crossed channels

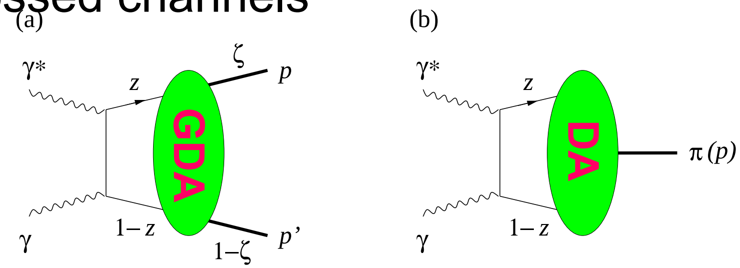

$\gamma^* \gamma \rightarrow p\ \text{pbar},\ \pi\pi,\ \rho\rho, \ldots$

generalised distribution amplitudes (GDAs) analogs of GPDs

- wide angle scattering

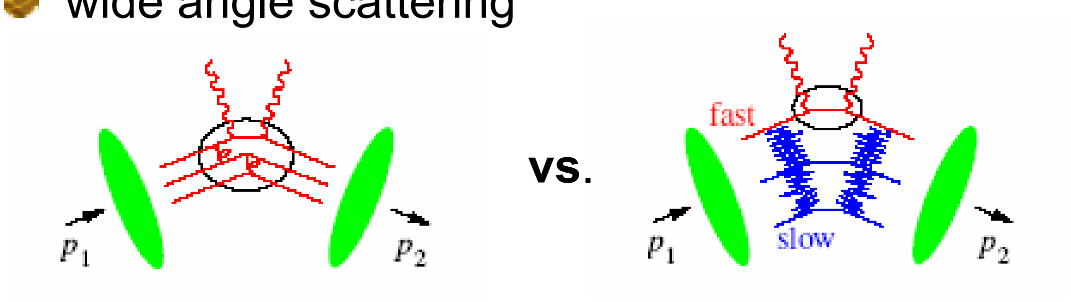

all invariants (*s, t, u*) large

$\gamma p \rightarrow \gamma p,\ \gamma^* \gamma \rightarrow p\ \text{pbar}, \ldots$

Theoretical Ansätze for GPDs:

- GPDs from double distributions: [Radyushkin 99, Polyakov/Weiss 99, . . .]
  - + polynomiality condition automatically fulfilled
  - − non-trivial t-dependence?
- GPDs from (light-cone) wave functions: [Diehl et al. 00, . . .]
  - + non-trivial (x, ξ, t) dependence
  - − only for large x, no polynomiality
- Non-trivial ξ-dependence via evolution [Shuvaev et al. 99]
- Constituent Quark Models [Scopetta/Vento 03, Pasquini et al. 04, . . .]
- . . .

For reviews see also:
[Goeke/Polyakov/Vanderhaeghen 01, Diehl 03, Belitsky/Radyushkin 05]

This Work: Diehl, Jakob, Feldmann and Kroll (2005)

- Valence quark GPDs at $\xi = 0$ from fit to elastic-form-factor data.

GPDs for valence quarks: (Ji's notation)

$$H_v^q(x,t,\mu^2) = H^q(x,\xi=0,t,\mu^2) + H^q(-x,\xi=0,t,\mu^2)$$
$$E_v^q(x,t,\mu^2) = E^q(x,\xi=0,t,\mu^2) + E^q(-x,\xi=0,t,\mu^2)$$

Related Nucleon Form Factors:

$$F_1^{p(n)}(t) = \int_0^1 dx \left(\frac{2}{3} H_v^{u(d)}(x,t,\mu^2) - \frac{1}{3} H_v^{d(u)}(x,t,\mu^2)\right)$$
$$F_2^{p(n)}(t) = \int_0^1 dx \left(\frac{2}{3} E_v^{u(d)}(x,t,\mu^2) - \frac{1}{3} E_v^{d(u)}(x,t,\mu^2)\right)$$

Strategy

- Qualitative behaviour from Regge phenomenology and physical intuition about impact-parameter GPDs.
- Compare different interpolations between small-x and large-x, assuming exponential t-dependence [default]:

$$H_v^q(x,t) := q_v(x)\exp[t f_q(x)]$$
$$E_v^q(x,t) := e_v^q(x)\exp[t g_q(x)]$$

- Forward limit $q_v(x)$ from standard PDFs. Positivity bounds constrain $e_v^q(x)$ (to some extent).
- Ansatz for forward limit: $e_v^q(x) \propto x^{-\alpha}(1-x)^{\beta_q}$ with $\alpha \approx 0.5$.

  Normalization: $\int_0^1 dx\, e_v^q(x) = \kappa_q$ (magn. moments, strange quarks neglected)
- Fit of profile functions $f_q(x)$ and $g_q(x)$ to electromagnetic proton and neutron form factors.

profile function

$$f_q(x) = -\alpha' (1-x)^3 \ln x + B_q (1-x)^3 + A_q x (1-x)^2$$

$$g_q(x) = -\alpha' (1-x)^3 \ln x + D_q (1-x)^3 + C_q x (1-x)^2$$

A_q, B_q fitted to F_1^p and F_1^n

C_q, D_q fitted to F_2^p and F_2^n

(fitting of α' optional)

shape of profile functions motivated by Regge phenomenology (small *x* and *t*)

assuming dominance of a single Regge pole:

$$H_v(x,t) \simeq \left(\frac{x_0}{x}\right)^{\alpha(0)} \exp\left[\left(\alpha' \log\frac{x_0}{x} + b_0 + \dots\right) t\right]$$

Results for $H_v^q(x,t)$

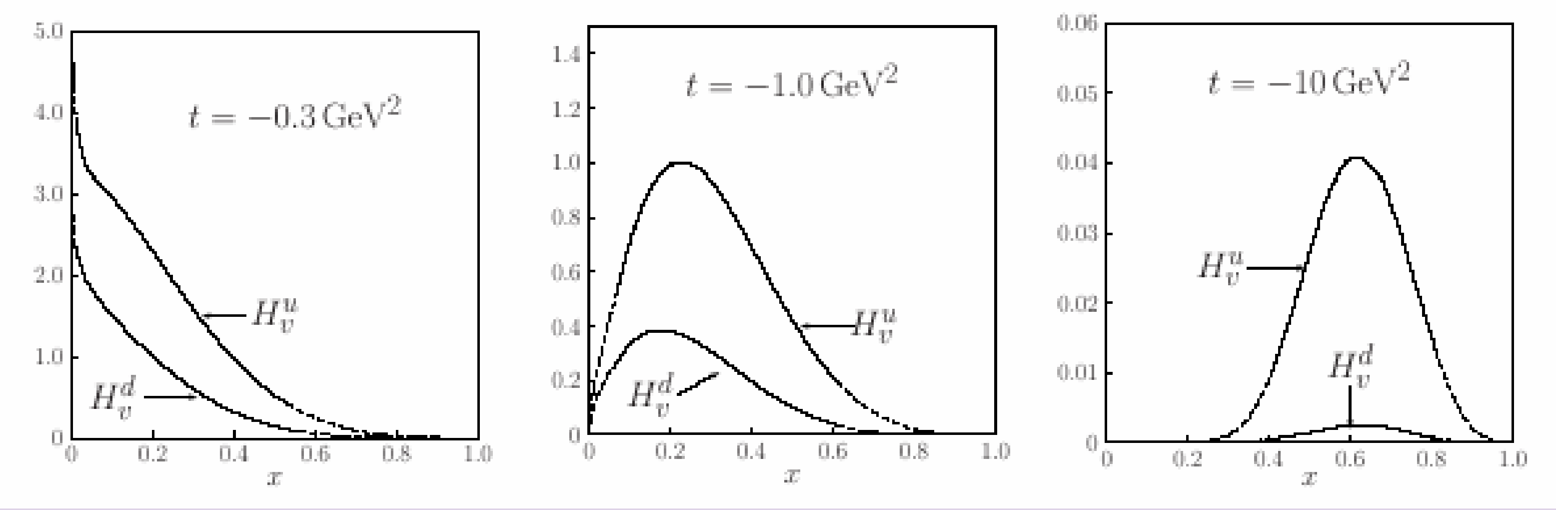

- small $|t|$: GPDs behave like PDFs
- large $|t|$: pronounced maximum at increasing values of x

OAM from QCD Lattice calculations

$$A_n^q(\Delta^2) = \int_0^1 dx\, x^{n-1} H^q(x,\Delta^2)$$

$$H^q(x,0) = q(x)$$

$$B_n^q(\Delta^2) = \int_0^1 dx\, x^{n-1} E^q(x,\Delta^2)$$

$$\tilde{A}_n^q(\Delta^2) = \int_0^1 dx\, x^{n-1} \tilde{H}^q(x,\Delta^2)$$

$$\tilde{H}^q(x,0) = \Delta q(x)$$

$$A_n^{Tq}(\Delta^2) = \int_0^1 dx\, x^{n-1} H^{Tq}(x,\Delta^2)$$

$$H^{Tq}(x,0) = \delta q(x)$$

↑ GFFs ↑ GPDs

$$\frac{1}{2}\left(A_2^q(0) + B_2^q(0)\right) = J^q$$

Ji

$$A_1^q(\Delta^2) = F_1^q(\Delta^2)$$

$$B_1^q(\Delta^2) = F_2^q(\Delta^2)$$

$$\tilde{A}_1^q(\Delta^2) = g_A^q(\Delta^2)$$

$$A_1^{Tq}(\Delta^2) = g_T^q(\Delta^2)$$

Note: here $H^q(x,\Delta^2) \equiv H^q(x,\xi=0,\Delta^2)$, etc.

OAM from QCD Lattice calculations

(Orbital) Angular Momentum

$$\frac{1}{2} = \underbrace{\frac{1}{2}\Delta\Sigma + L^q}_{J^q} + J^g\,, \quad \Delta\Sigma = \sum_q \Delta q$$

$$\text{EMT}: J^q = \frac{1}{2}\left(A_2^q(0) + B_2^q(0)\right)$$

$\beta = 5.40, \kappa_{sea} = 0.1350$

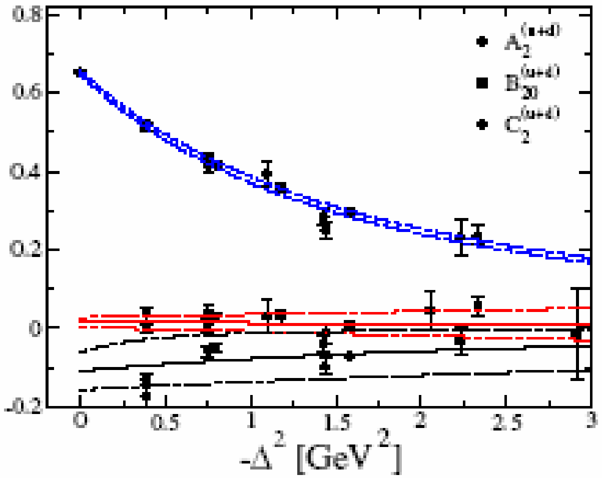

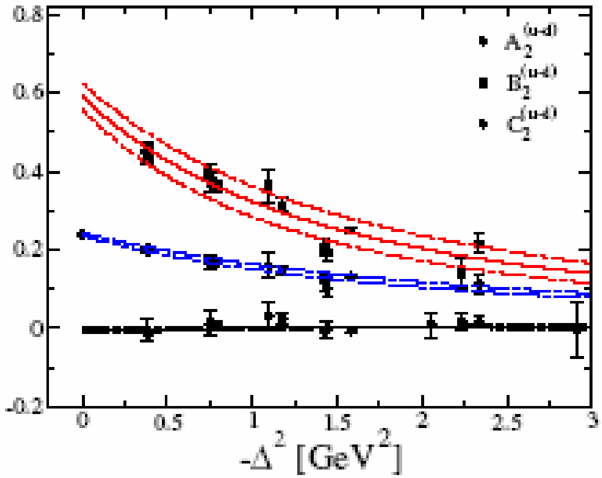

$$A_2(\Delta^2) = \frac{A_2(0)}{(1 - \Delta^2/M_2^2)^2}$$

$$B_2(\Delta^2) = \frac{B_2(0)}{(1 - \Delta^2/\hat{M}_2^2)^2}$$

QCD Lattice calculations

Chiral extrapolation

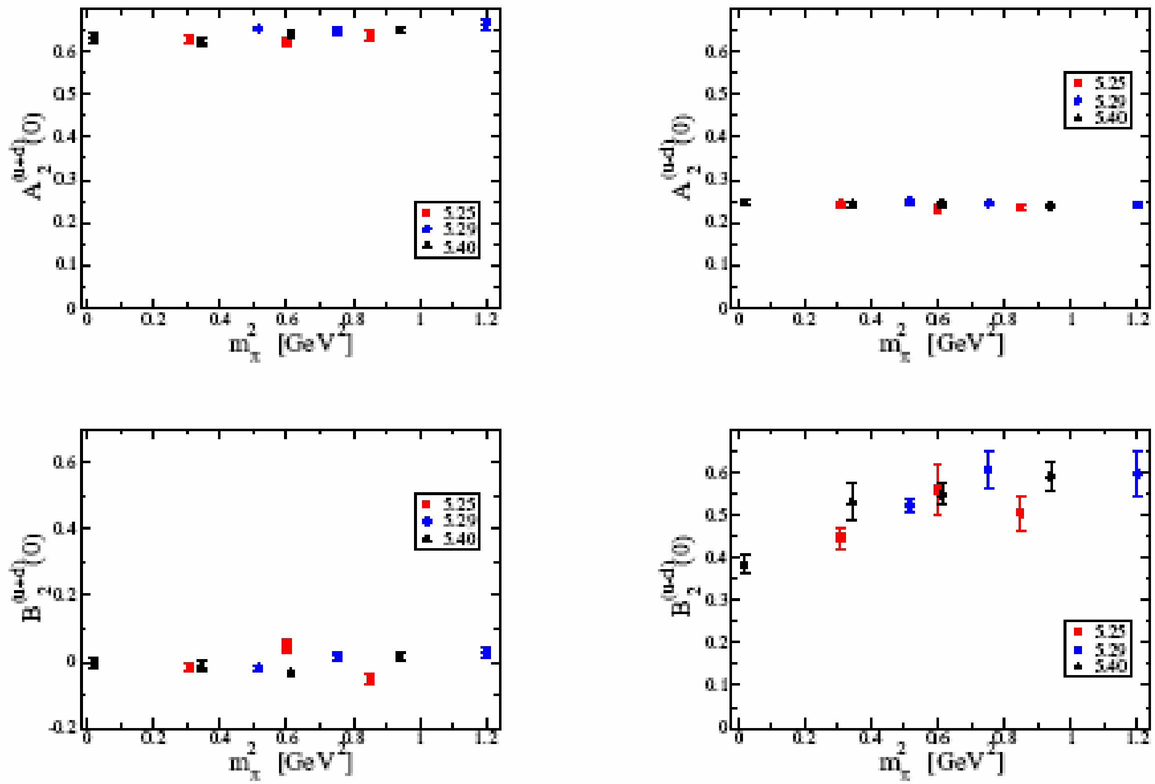

$$J^{u+d} \approx \frac{1}{2} \langle x \rangle^{u+d}$$

$$J^{u-d} \approx \frac{5}{4} \langle x \rangle^{u-d}$$

$$J^q = L^q + S^q, \quad S^q = \frac{1}{2}\Delta q$$

from QCDSF Collaboration (Lattice)

$$J^u = 0.32(4), \quad J^d \approx 0$$

$$L^u = -0.21(4), \quad L^d = 0.24(4)$$

$\overline{MS}$, $Q^2 = 4$ GeV^2

$$L^{u+d} = 0.03(7)$$

↑

Valence quarks only

$$L^{u-d} = -0.45(6)$$

$\cdots$ but strong cancellations

$$B_1^{u+d} \approx B_2^{u+d} \approx 0 \quad \Longrightarrow E^{u+d} \approx 0$$

Diehl, Jakob, Feldmann and Kroll (2005)

from fits to nucleon formfactors

$$J^u = 0.20 \div 0.23 \qquad J^d = -0.04 \div 0.04$$

$$L^{u+d} = -(0.06 \div 0.11)$$

$$L^{u-d} = -(0.39 \div 0.41)$$

Deeply Virtual Compton Scattering $e\,p \to e\,p\,\gamma$

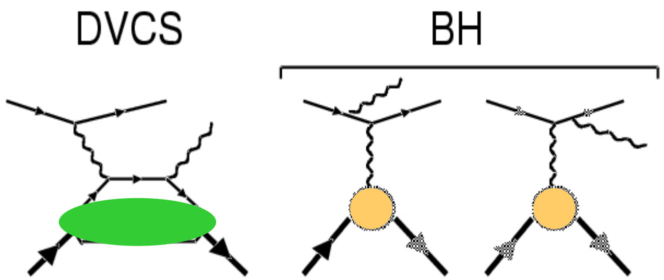

The same final state in DVCS and Bethe-Heitler

$$\sigma \propto |T_{BH}|^2 + |T_{DVCS}|^2 + \left(T_{BH}T^*_{DVCS} + T^*_{BH}T_{DVCS}\right)$$

interference $\mathcal{I}$

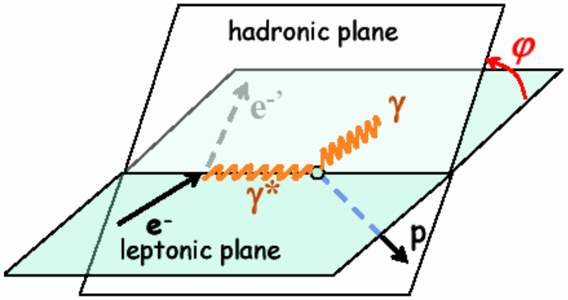

up to twist-3
BMK (2002)

$$|\mathcal{T}_{\rm DVCS}|^2 = \frac{e^6}{y^2 Q^2}\left\{c_0^{\rm DVCS} + \sum_{n=1}^{2}\left[c_n^{\rm DVCS}\cos(n\phi) + s_n^{\rm DVCS}\sin(n\phi)\right]\right\}$$

$$\mathcal{I} = \frac{\pm e^6}{x_{\rm B}y^3\Delta^2\mathcal{P}_1(\phi)\mathcal{P}_2(\phi)}\left\{c_0^{\mathcal{I}} + \sum_{n=1}^{3}\left[c_n^{\mathcal{I}}\cos(n\phi) + s_n^{\mathcal{I}}\sin(n\phi)\right]\right\},$$

$\mathcal{P}_1(\Phi)$, $\mathcal{P}_2(\Phi)$
BH propagators

c_i^{DVCS}, s_i^{DVCS}, $c_i^{\mathcal{I}}$, $s_i^{\mathcal{I}}$ depend on spin orientations of lepton and nucleon

Fourier coefs with twist-2 DVCS amplitudes (related to GPDs)
c_0^{DVCS}, $c_1^{\mathcal{I}}$, $s_1^{\mathcal{I}}$ and $c_0^{\mathcal{I}}$ (the last one Q suppresed)

interference + structure of azimuthal distributions + Q^2 dependence

a powerful tool to disantangle leading- and higher-twist effects and extract DVCS amplitudes including their phases

Available experimental data on DVCS (1)

- lepton charge or single spin asymmetries at moderate and large x_B

HERMES and JLAB results

- beam-charge asymmetry $A_C(\varphi)$

$$d\sigma(e^+,\phi) - d\sigma(e^-,\phi) \propto \mathrm{Re}[F_1 \mathcal{H}] \cdot \cos\phi$$

- beam-spin asymmetry $A_{LU}(\varphi)$

$$d\sigma(\vec{e},\phi) - d\sigma(\overleftarrow{e},\phi) \propto \mathrm{Im}[F_1 \mathcal{H}] \cdot \sin\phi$$

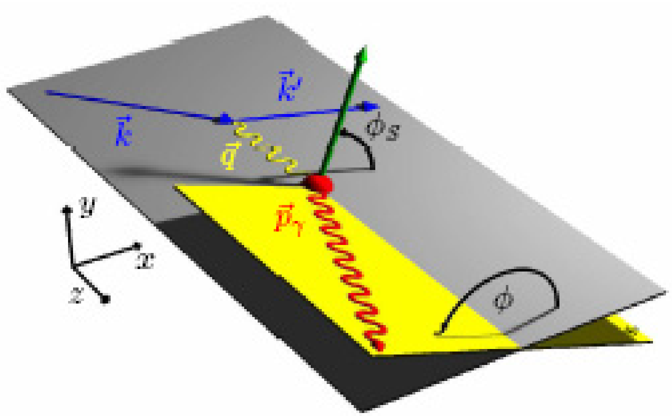

- longitudinal target-spin asymmetry $A_{UL}(\varphi)$

$$d\sigma(\overleftarrow{P},\phi) - d\sigma(\vec{P},\phi) \propto \mathrm{Im}[F_1 \widetilde{\mathcal{H}}] \cdot \sin\phi$$

- transverse target-spin asymmetry $A_{UT}(\varphi,\varphi_s)$

$$d\sigma(\phi,\phi_S) - d\sigma(\phi,\phi_S+\pi) \propto \mathrm{Im}[F_2\mathcal{H} - F_1\mathcal{E}] \cdot \sin(\phi-\phi_S)\cos\phi + \mathrm{Im}[F_2\widetilde{\mathcal{H}} - F_1\xi\widetilde{\mathcal{E}}] \cdot \cos(\phi-\phi_S)\sin\phi$$

F_1 and F_2 are Dirac and Pauli proton form factors

Beam SSA after correction for π^0 contamination from CLAS

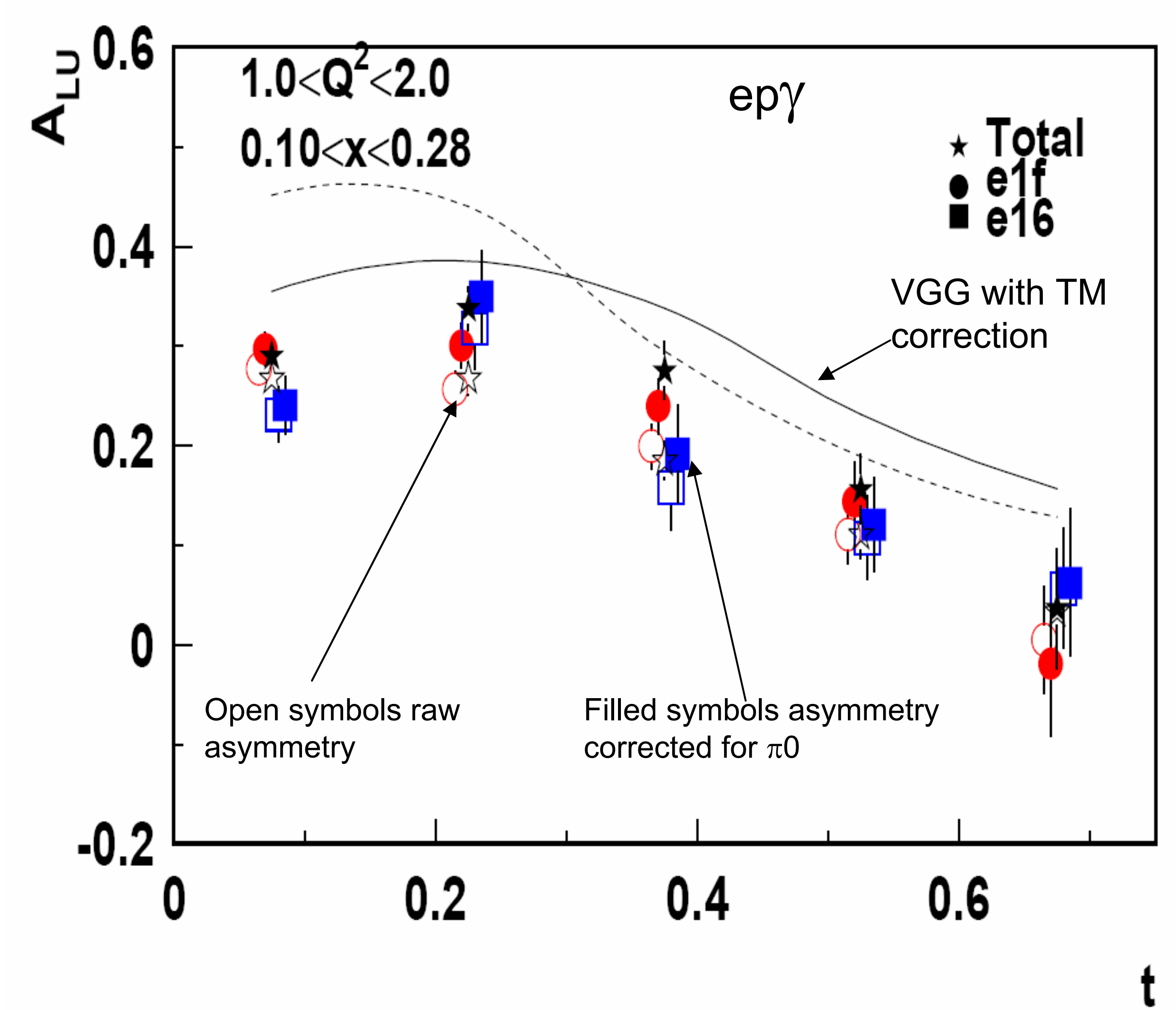

Two data sets (e16 at 5.7 GeV,e1f at 5.5 GeV) with different torus field (different kinematic coverage) and beam energy are consistent.

Transverse Target-Spin Asymmetry from HERMES

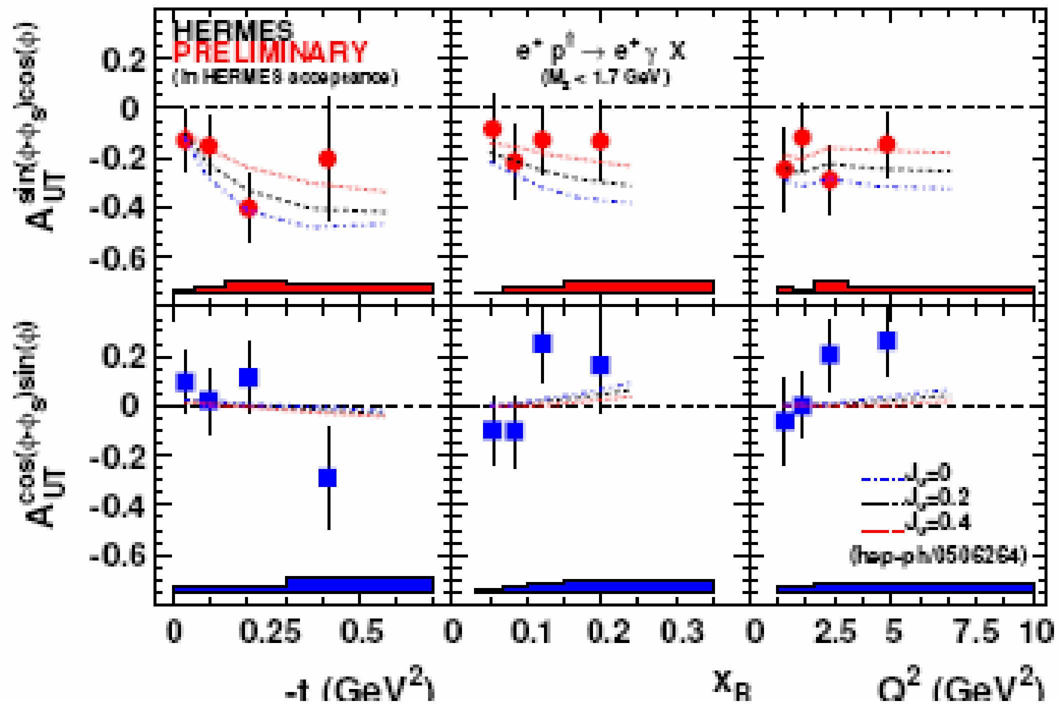

$\propto \mathrm{Im}[F_2\mathcal{H} - F_1\mathcal{E}]$

$\propto \mathrm{Im}[F_2\widetilde{\mathcal{H}} - F_1\xi\widetilde{\mathcal{E}}]$

- Goeke et al., Prog.Part.Nucl.Phys.47 (2001) 401: The nucleon-helicity flip GPD E in the forward limit is modeled by $e(x) = A \cdot q_{val}(x) + B \cdot \delta(x)$, according to χQSM model. The values A and B are related to J_q by: $\int dx\, x[q(x) + e(x)] = J_q$, $\int dx\, e(x) = F_2^q(0) = k^q$.

A Model-Dependent Constraint on J_u vs J_d

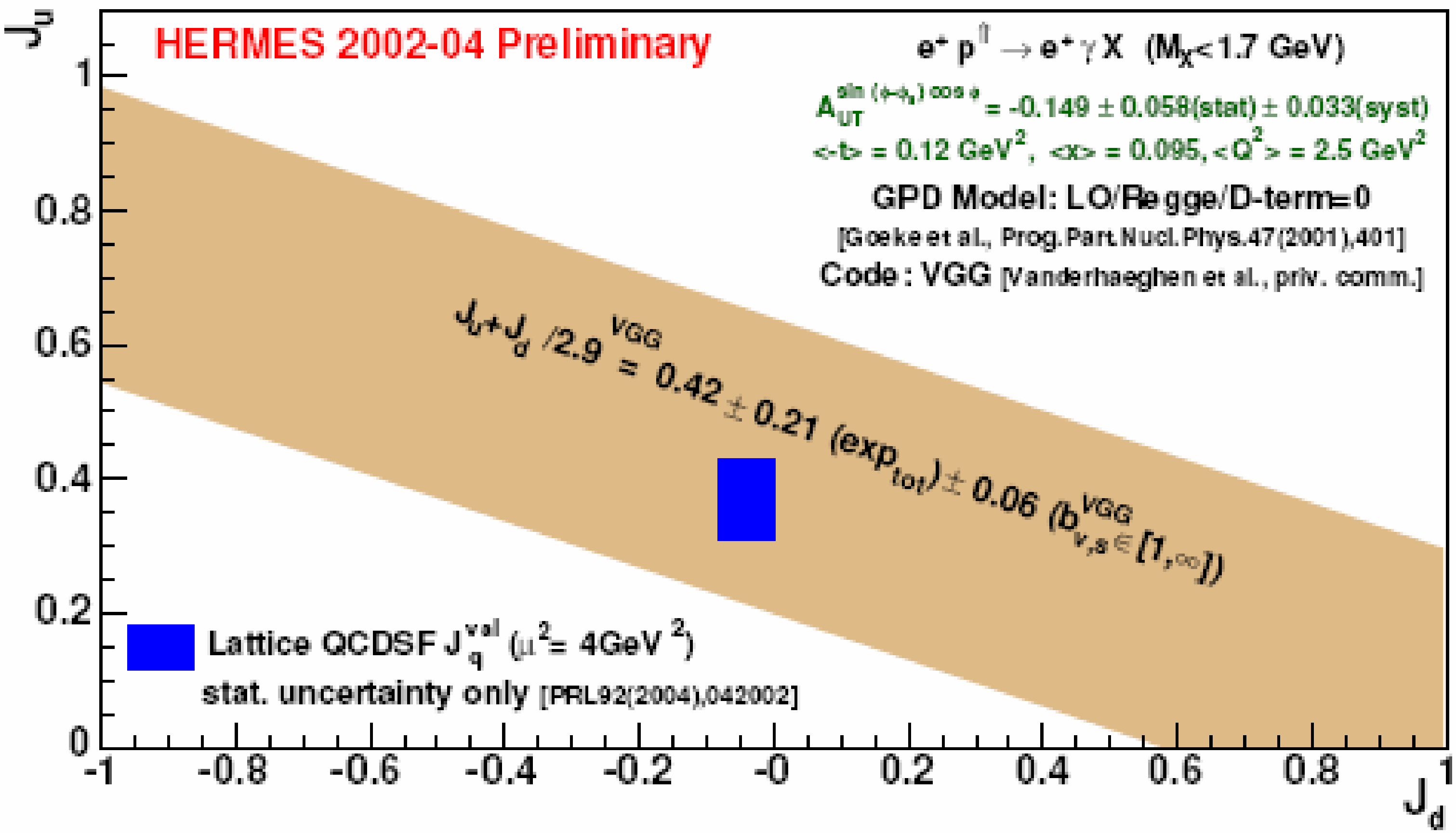

- The quenched Lattice calculation was done with the the pion masses 1070, 870, and 640 MeV, and extrapolated linearly in m_π^2 to the physical value.

Available experimental data on DVCS (2)

- cross section σ_{DVCS} averaged over φ for unpolarised protons H1 and ZEUS

at small x_B (< 0.01) $\sigma^{unp}_{DVCS} \propto 4(\mathcal{H}\mathcal{H}^* + \widetilde{\mathcal{H}}\widetilde{\mathcal{H}}^*) - 2\frac{t}{4M^2}\mathcal{E}\mathcal{E}^*$ → H^{sea}, H^g

Q² dependence: NLO predictions

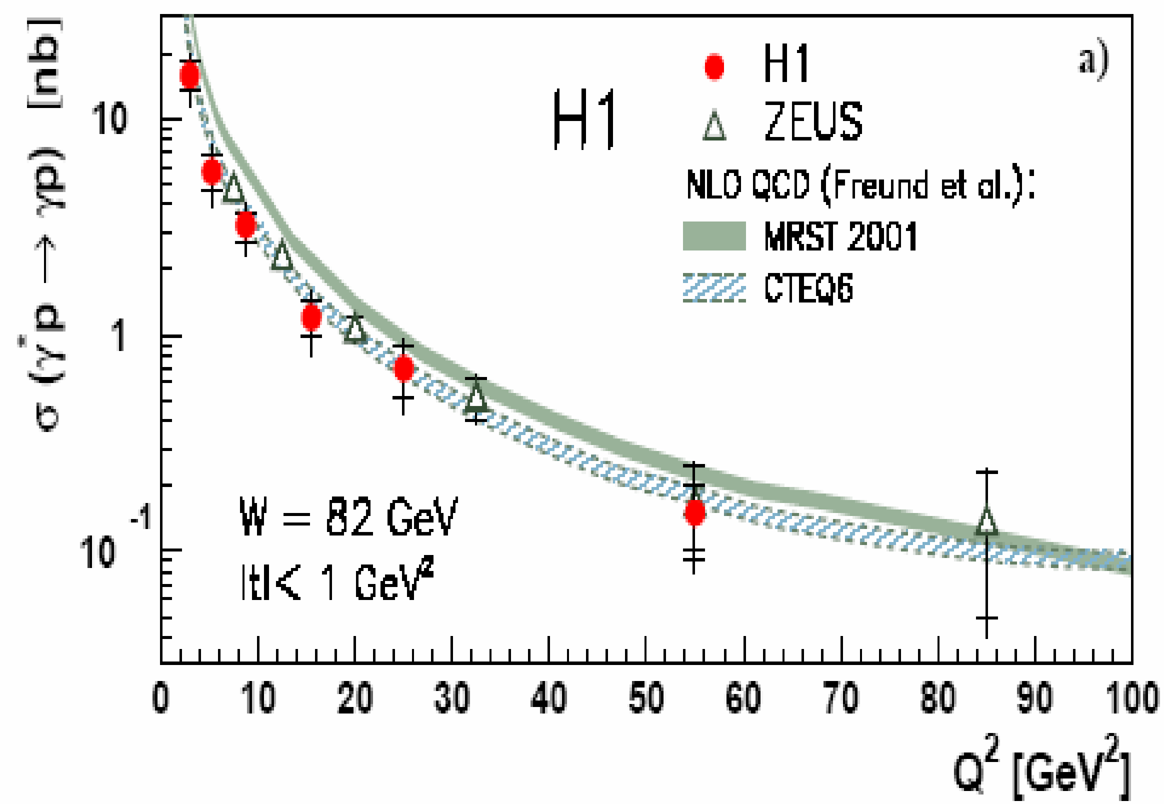

b assumed Q²-independent

no intrinsic skewing

bands reflect experimental error on *b*: 5.26 < b < 6.40

- **Wide range of Q² - sensitivity to QCD evolution of GPDs**
- **Difference between MRS/CTEQ due to different xG at low x_B**

W dependence: NLO predictions

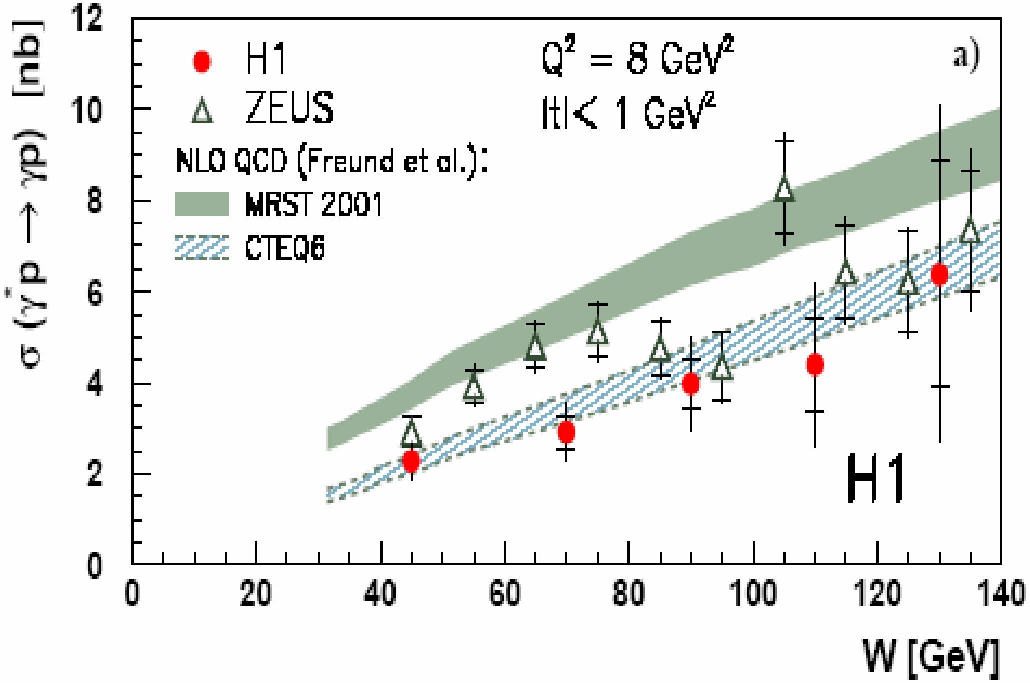

1996-2000

Meaurements of *b* significantly constrain uncertainty of models

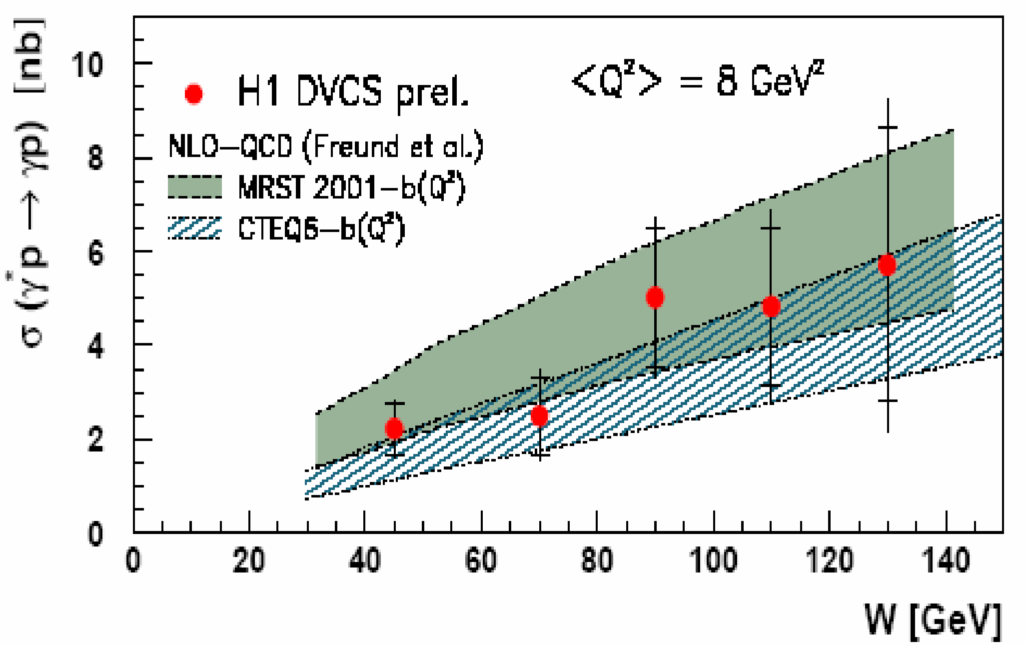

Older H1 (prel.) measurement on 2000 data with a ***b*** value in the range [**4 - 7**] GeV^{-2}

Impact parameter representation and probabilistic interpretation

Generically

$$A_n^q(\mathbf{b}_\perp^2) = \int \frac{d^2\boldsymbol{\Delta}_\perp}{(2\pi)^2} e^{i\,\mathbf{b}_\perp \boldsymbol{\Delta}_\perp} A_n^q(\boldsymbol{\Delta}_\perp^2) \quad \Longleftrightarrow \quad \boxed{\langle p_+, s|\bar{q}(\mathbf{b}_\perp)\cdots q(\mathbf{b}_\perp)|p_+, s\rangle}$$

$$|p_+, s\rangle = \mathcal{N} \int \frac{d^2\mathbf{p}_\perp}{(2\pi)^2} |p_+, \mathbf{p}_\perp, s\rangle$$

$$H^q(x, \mathbf{b}_\perp^2) = \int \frac{d^2\boldsymbol{\Delta}_\perp}{(2\pi)^2} e^{i\,\mathbf{b}_\perp \boldsymbol{\Delta}_\perp} H^q(x, \boldsymbol{\Delta}_\perp^2)$$

Note: here $H^q(x,\Delta^2) \equiv H^q(x,\xi=0,\Delta^2)$

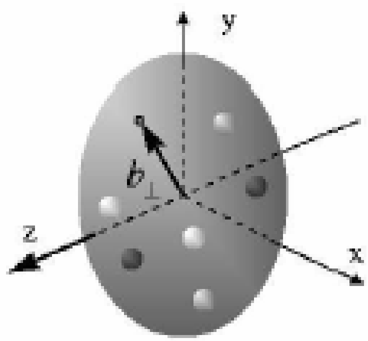

$F_1(\mathbf{b}_\perp^2) \equiv A_1(\mathbf{b}_\perp^2)$

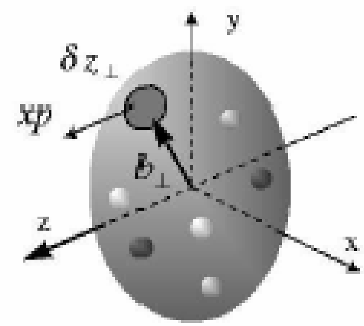

$H(x, \mathbf{b}_\perp^2)$

$\Longrightarrow$ Probability interpretation Burkardt

Key quantities

- Form factor

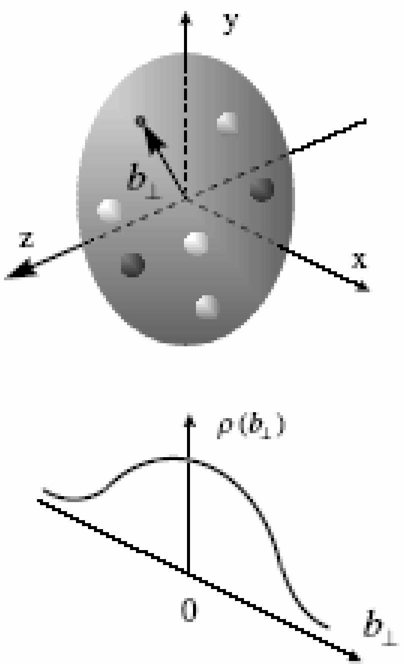

- Parton density

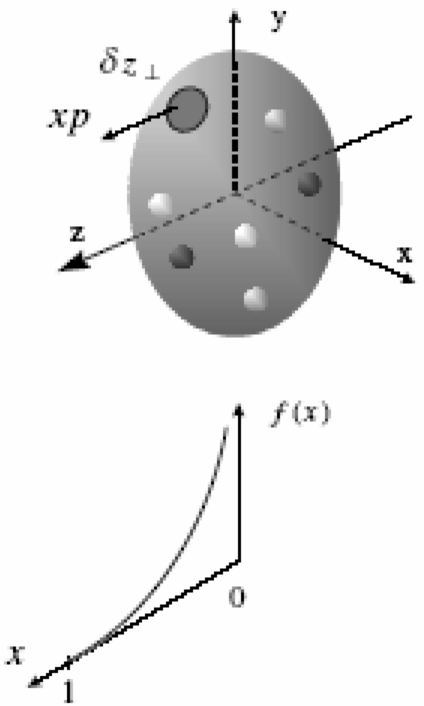

- Generalized parton distribution at η=0

$(\eta \equiv \xi)$

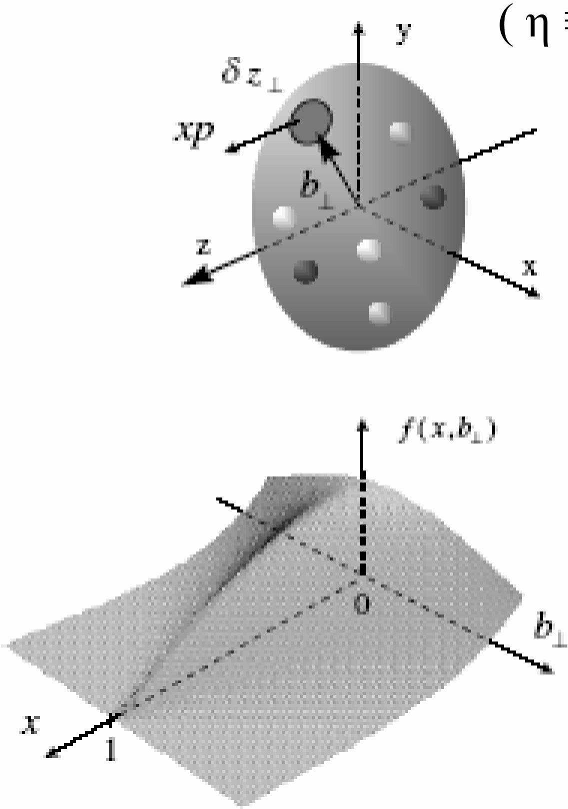

Spatial resolution: $\delta z_\perp \sim 1/Q$

5.2 Nucleon tomography from default fit to $F_{1,2}^{p,n}$

valence quarks: unpolarized

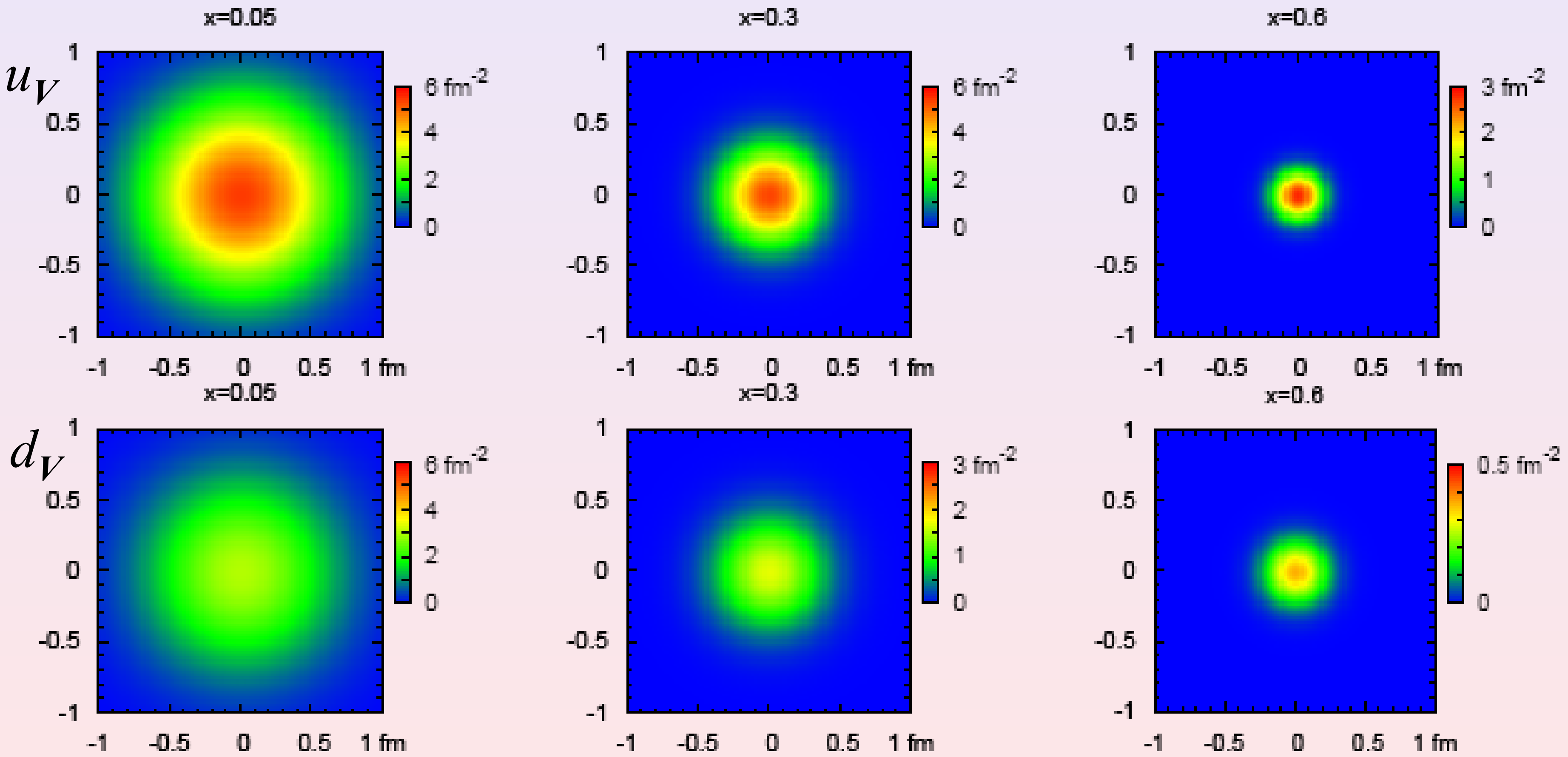

Nucleon tomography from default fit to $F_{1,2}^{p,n}$

valence quarks: in ⊥ polarized proton (sizeable systematic uncertainties!)

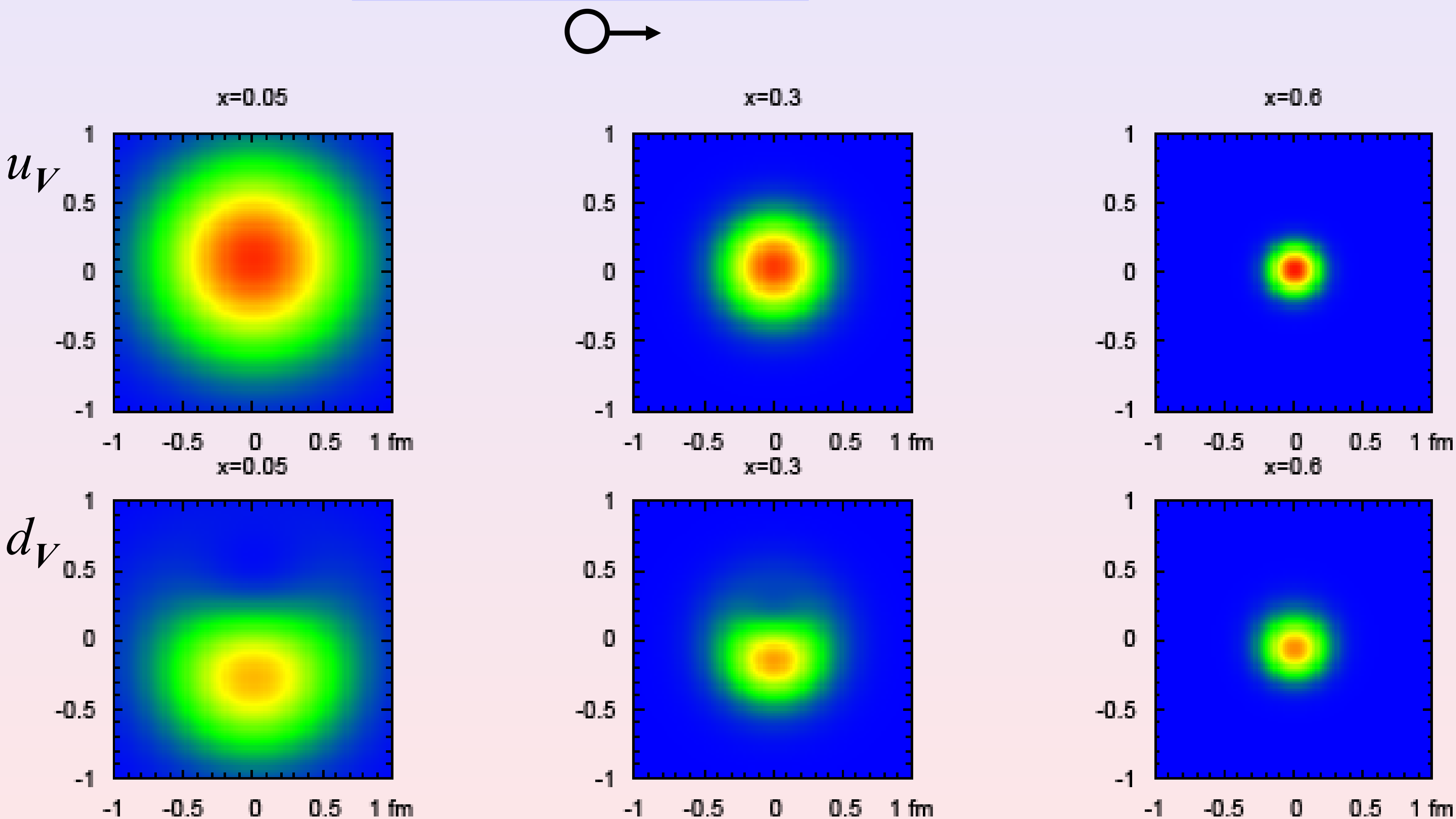

Deformation of quark space distribution in transversely polarised nucleon

$$q(x,\vec{b}_\perp)_{p\uparrow} = H(x,\vec{b}_\perp) - \frac{1}{2M}\frac{\partial}{\partial b_y}\int \frac{d^2\boldsymbol{\Delta}_\perp}{(2\pi)^2} E(x,0,-\boldsymbol{\Delta}_\perp^2) e^{-i\mathbf{b}_\perp\cdot\boldsymbol{\Delta}_\perp}$$

Intuitive connection with $\vec{L}_q$

- Electromagnetic interaction couples to vector current. Due to kinematics of the DIS-reaction (and the choice of coordinates — $\hat{z}$-axis in direction of the momentum transfer) the virtual photons "see" (in the Bj-limit) only the $j^+ = j^0 + j^z$ component of the quark current
- If up-quarks have positive orbital angular momentum in the $\hat{x}$-direction, then j^z is positive on the $+\hat{y}$ side, and negative on the $-\hat{y}$ side

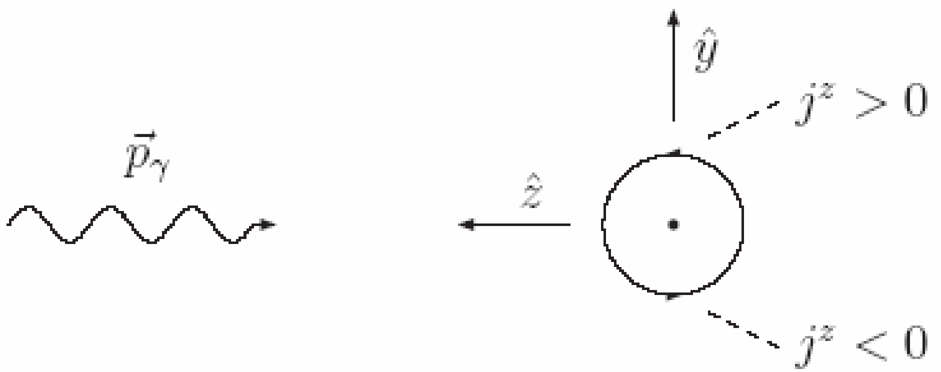

note: *j* denotes current (not angular momentum)

Final-state interactions

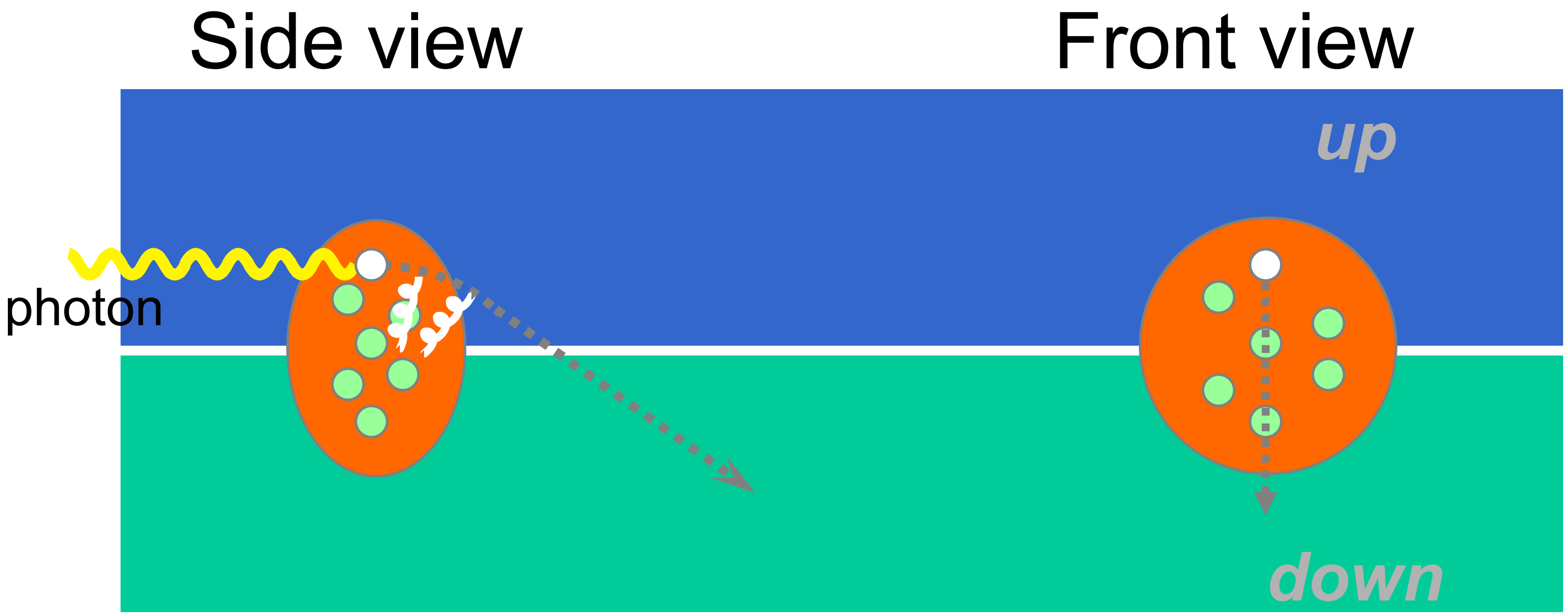

NOTE: QCD tells us that the FSI has to be attractive, since quark and remnants form a color antisymmetric state

Chromodynamic lensing

Sievers effect

- Deformation of quark distribution in transversely polarised nucleon

and

- Final state interaction

⬇

k_T asymmetry of ejected (unpolarised) quarks

Sivers: distribution of **unpol.** quarks in ⊥ pol. proton

$$f_{q/p^\uparrow}(x, \mathbf{k}_\perp) = f_1^q(x, \mathbf{k}_\perp^2) - f_{1T}^{\perp q}(x, \mathbf{k}_\perp^2) \frac{(\hat{\mathbf{P}} \times \mathbf{k}_\perp) \cdot S}{M}$$

Azimuthal Single-Spin Asymmetries

$$A_{UT}(\phi,\phi_S) = \frac{1}{\langle|S_\perp|\rangle}\frac{N_h^\uparrow(\phi,\phi_S)-N_h^\downarrow(\phi,\phi_S)}{N_h^\uparrow(\phi,\phi_S)+N_h^\downarrow(\phi,\phi_S)}$$

$$\sim \sin(\phi+\phi_S)\sum_q e_q^2\,\mathcal{I}\left[\frac{p_T\widehat{P}_{h\perp}}{M_h}h_1^q(x,k_T^2)H_1^{\perp,q}(z,p_T^2)\right]$$

$$+ \sin(\phi-\phi_S)\sum_q e_q^2\,\mathcal{I}\left[\frac{k_T\widehat{P}_{h\perp}}{M}f_{1T}^{\perp,q}(x,k_T^2)D_1^q(z,p_T^2)\right]$$

$$+ \cdots$$

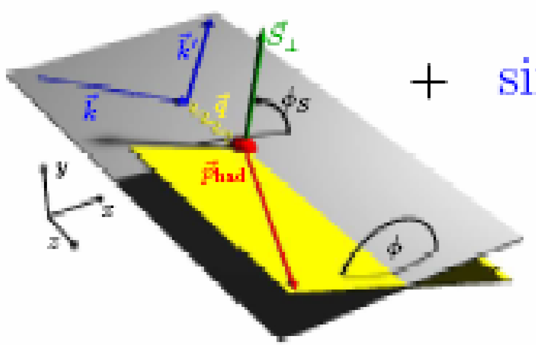

$\mathcal{I}[\ldots]$: convolution integral over k_T and p_T

$\Rightarrow$ 2D-fit of A_{UT} to get Collins and Sivers asymmetries:

$$A_{UT}(\phi,\phi_S) = 2\left\langle\sin(\phi-\phi_S)\right\rangle_{UT}\sin(\phi-\phi_s) + 2\left\langle\sin(\phi+\phi_S)\right\rangle_{UT}\sin(\phi+\phi_s)$$

comparison with HERMES

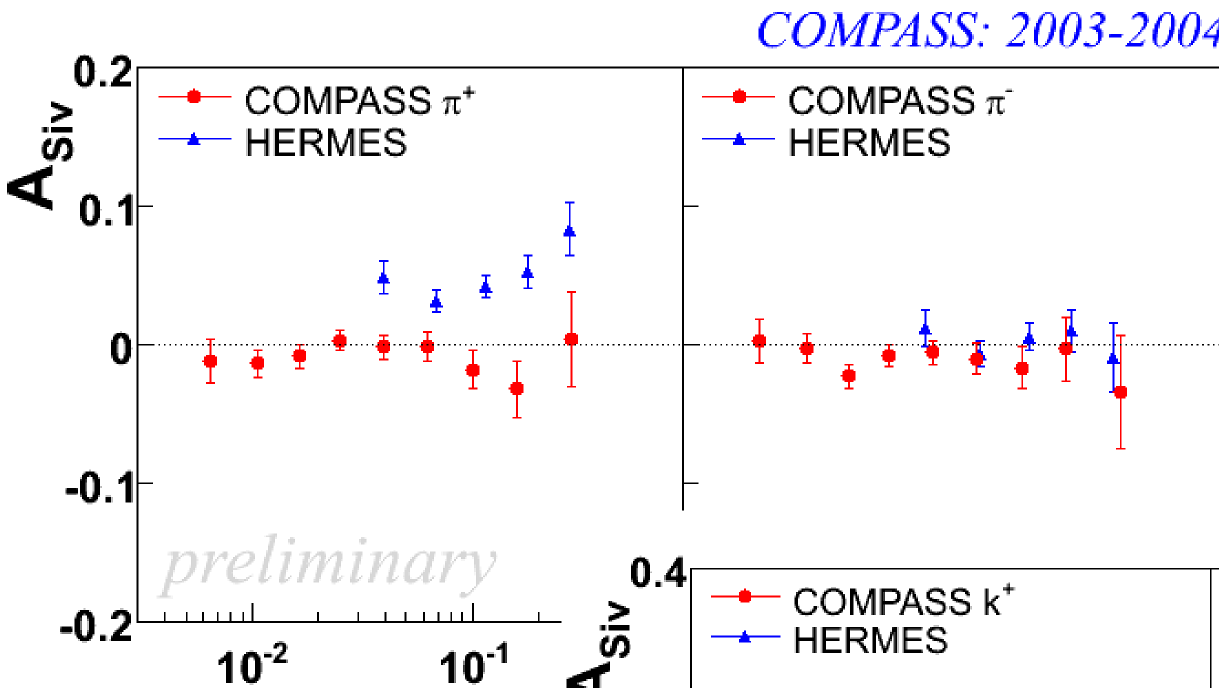

identified π's and K's

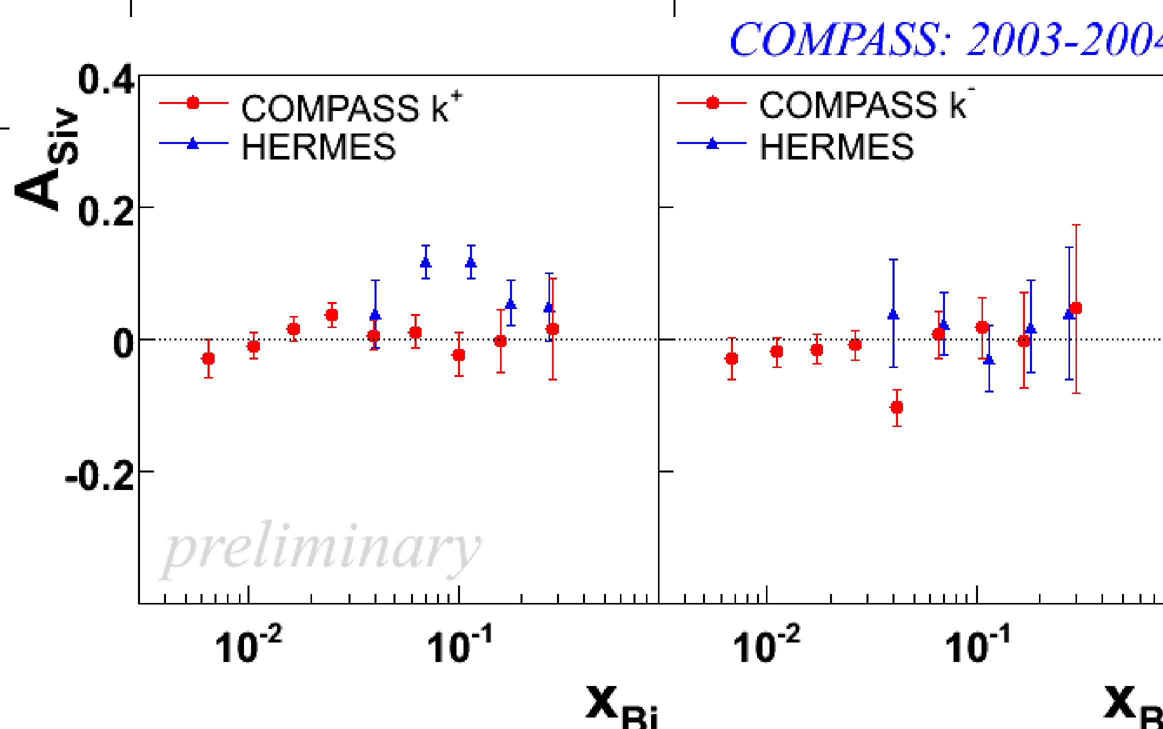

COMPASS – pol. deuterons

HERMES – pol. protons

Selected projects of future DVCS measurements

CLAS12 - DVCS/BH Target Asymmetry

$e\,p^{\uparrow} \longrightarrow ep\gamma$

Transversely polarized target

Sample kinematics

E = 11 GeV

Q^2=2.2 GeV^2, x_B = 0.25, -t = 0.5GeV^2

$\Delta\sigma_{UT} \sim \sin\phi \mathrm{Im}\{k_1(F_2 H - F_1 E) + \ldots\}d$

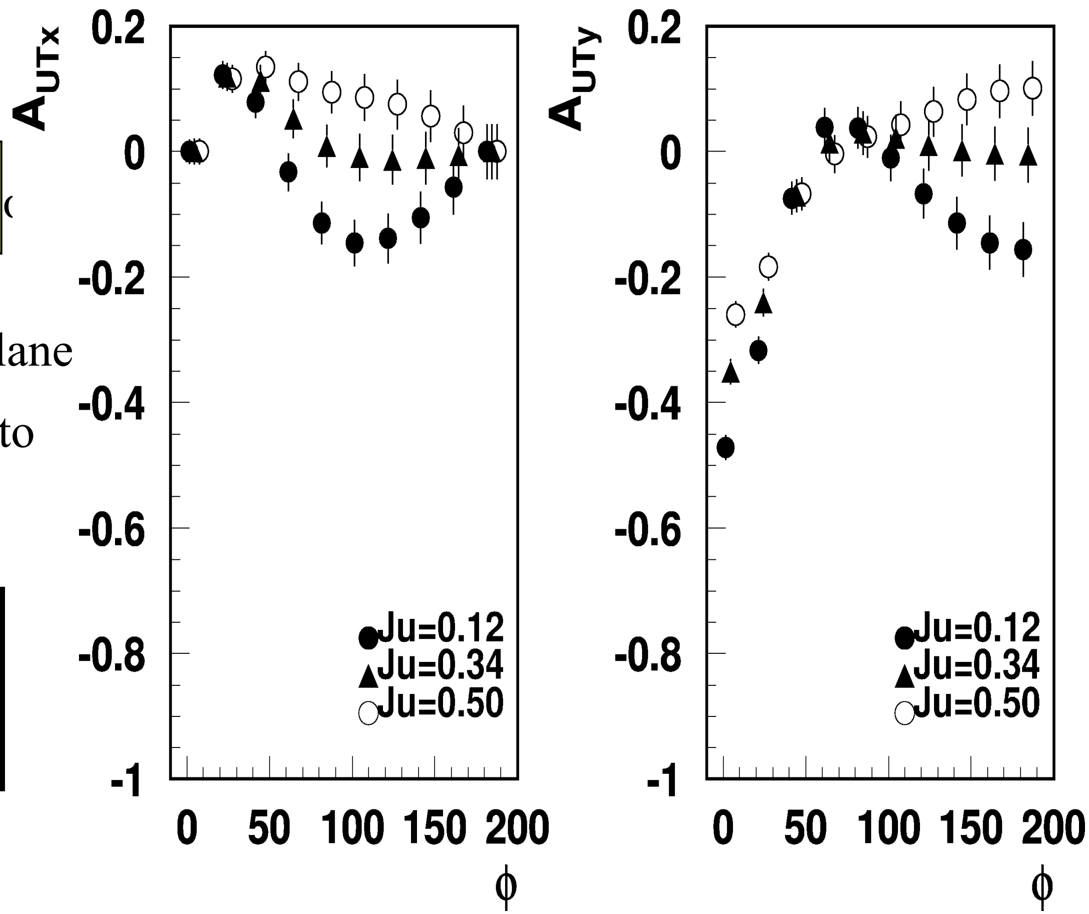

A_{UTx} Target polarization in scattering plane

A_{UTy} Target polarization perpendicular to scattering plane

- Asymmetry highly sensitive to the u-quark contributions to the proton spin.

Recoil detector design

"COMPASS+"

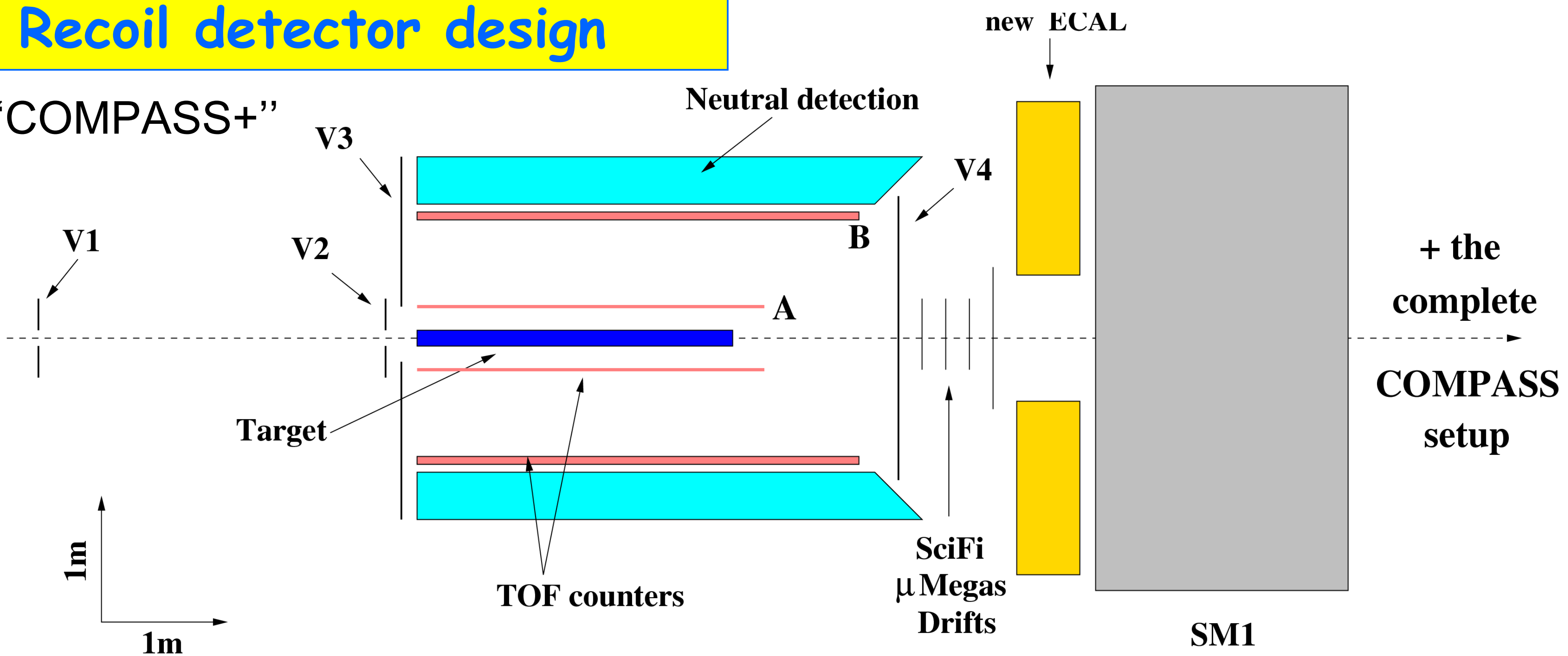

Goals: Detect protons of 250-750 MeV/c

t resolution => σ_{TOF} = 200 ps

exclusivity => Hermetic detector

Design :

2 concentric barrels of 24 scintillators counters read at both sides

European funding (127 k€) through a JRA for studies and construction of a prototype (Bonn, Mainz, Saclay, Warsaw)

Experimental set-up for the recoil prototype test run in 2006

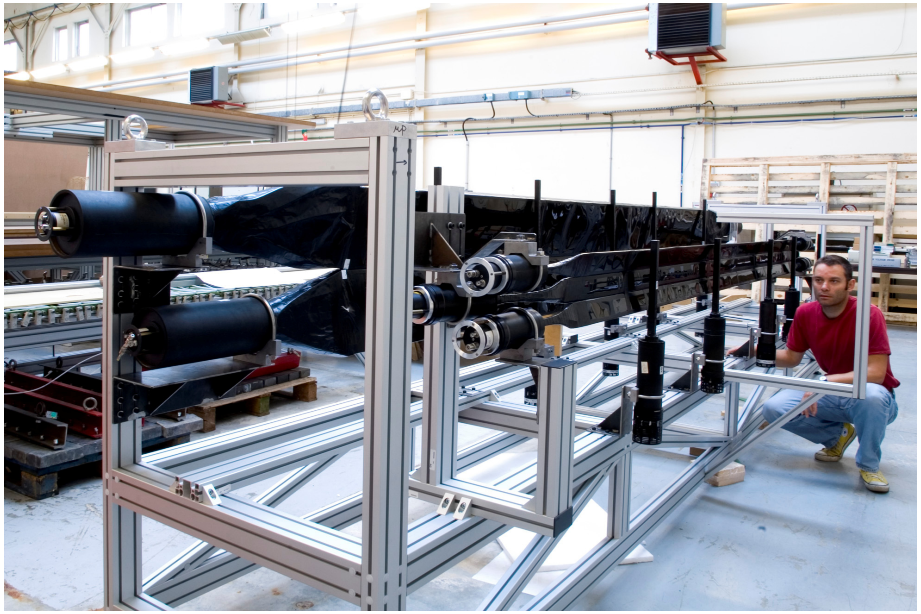

All scintillators are BC 408

A: 284cm x 6.5cm x 0.4cm
Equiped with XP20H0 (screening grid)

B: 400cm x 29cm x 5cm
Equiped with XP4512

Resolution on TOF
Center 340ps HV low
Center 310ps HV high
Expected resolution 280 ps

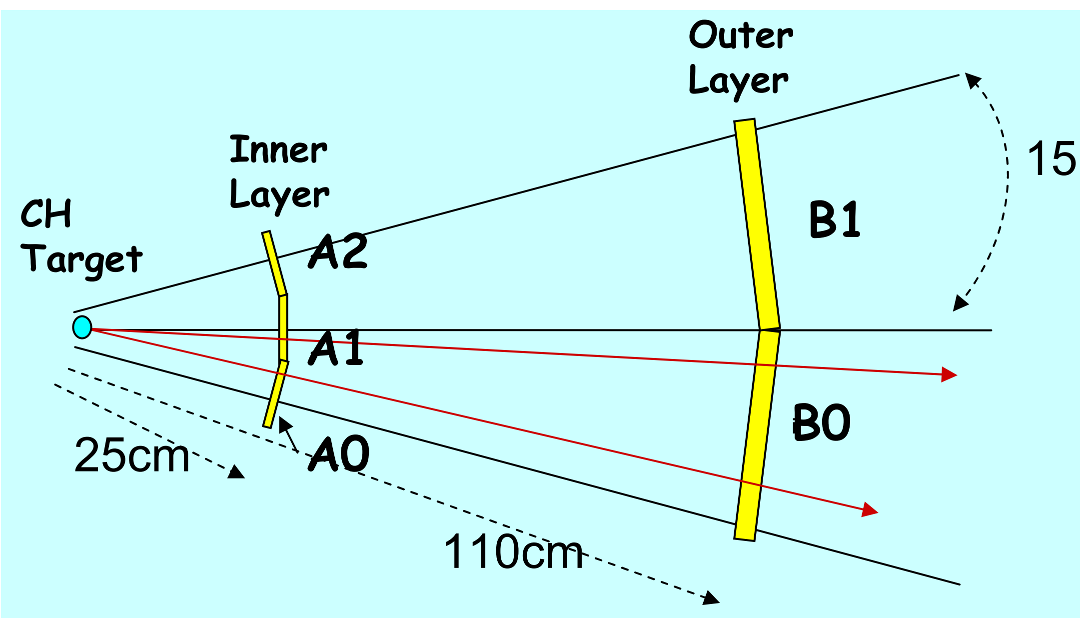

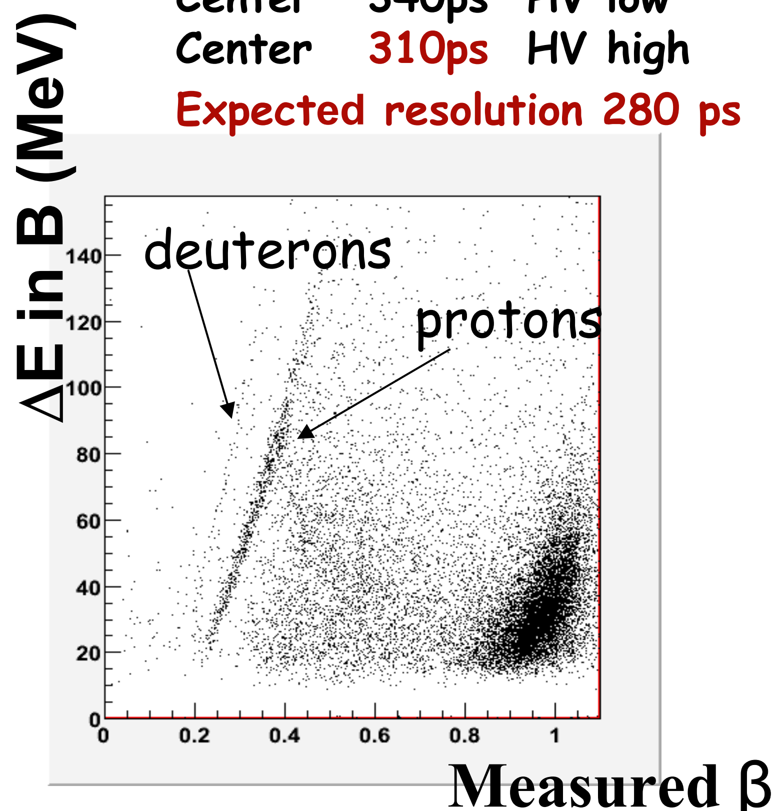

Projected errors of a planned DVCS experiment at CERN

Beam Charge Asymmetry

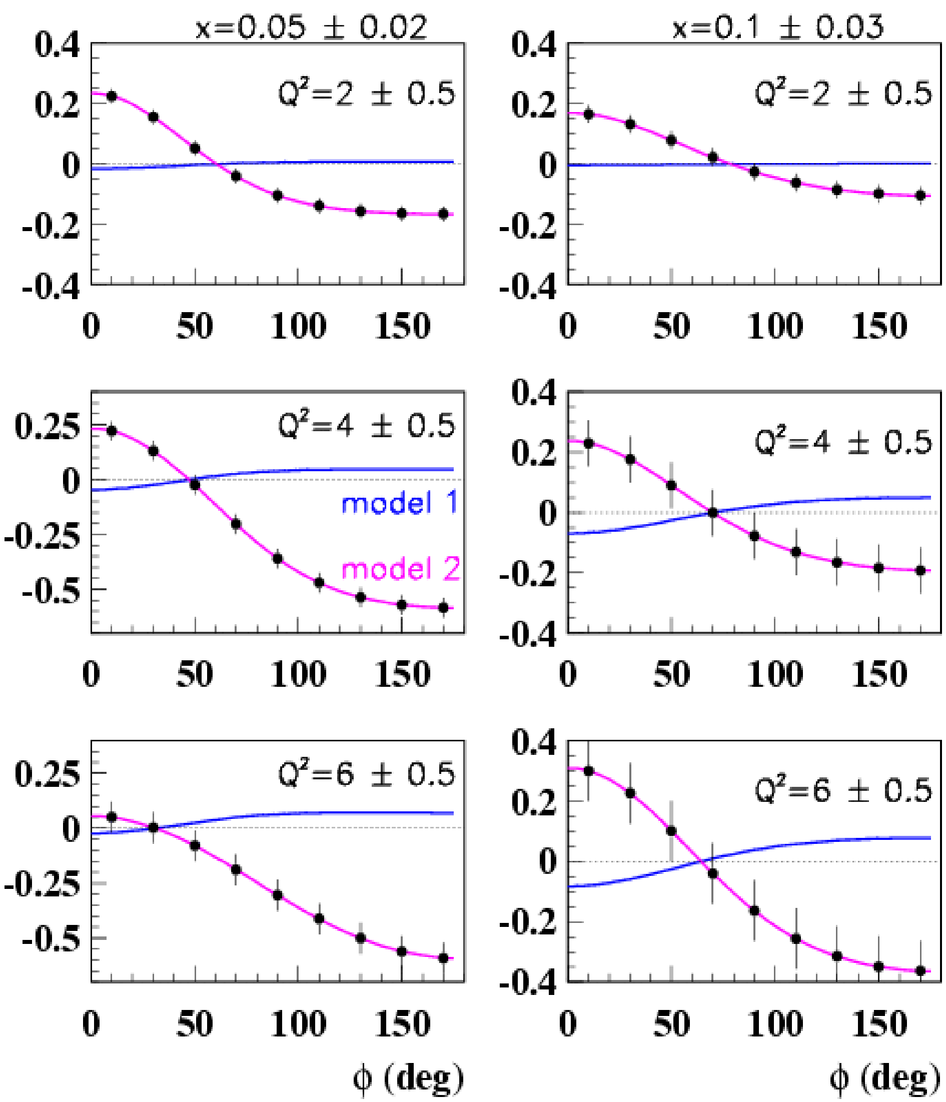

$\mathcal{L}$ = 1.3 10^{32} cm^{-2} s^{-1}

E_{beam} = 100 GeV
6 month data taking
25 % global efficiency

6/18 (x,Q^2) data samples

3 bins in x_{Bj}= 0.05, 0.1, 0.2
6 bins in Q^2 from 2 to 7 GeV^2

Model 1 : $H(x,\xi,t) \sim q(x)\,F(t)$

Model 2 : $H(x,0,t) = q(x) / x^{\alpha' t}$

Good constrains for models

eRHIC ring-ring design

- Collisions at 12 o'clock interaction region
- 10 GeV, 0.5 A e-ring with 1/3 of RHIC circumference
- Inject at full energy 5 - 10 GeV
- Existing RHIC interaction region allows for typical asymmetric detector (similar to HERA or PEP II detectors)

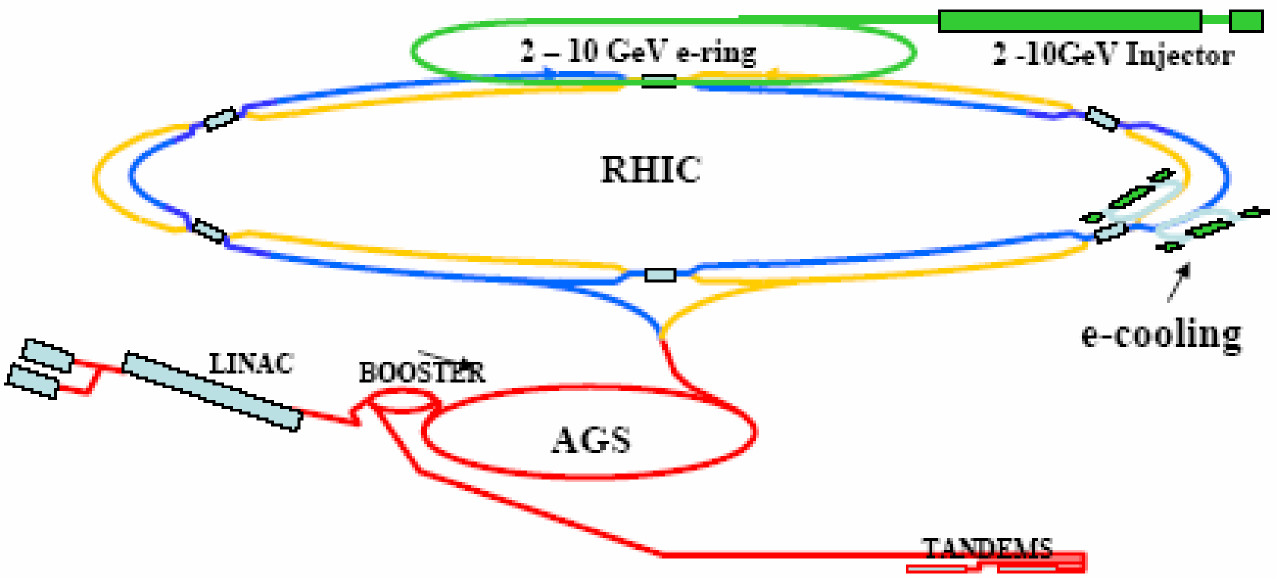

Precision of DVCS unpolarized cross sections at eRHIC

HE setup: $e^{+/-}$ **(10 GeV) + p (250 GeV)** $\mathcal{L}$ **= 4.4 · 10^{32} $cm^{-2}s^{-1}$ 38 pb^{-1}/day**

For one out of 6 W intervals (30 < W < 45 GeV)

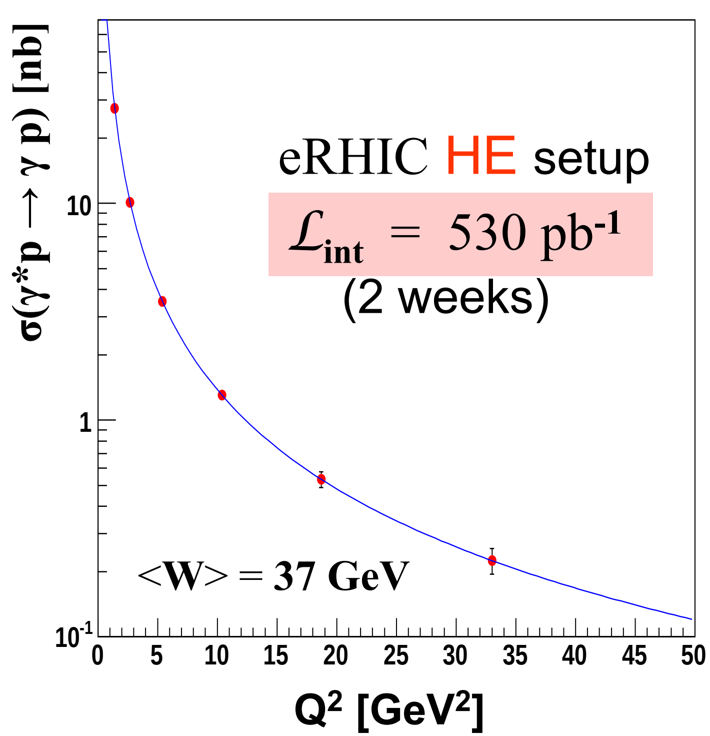

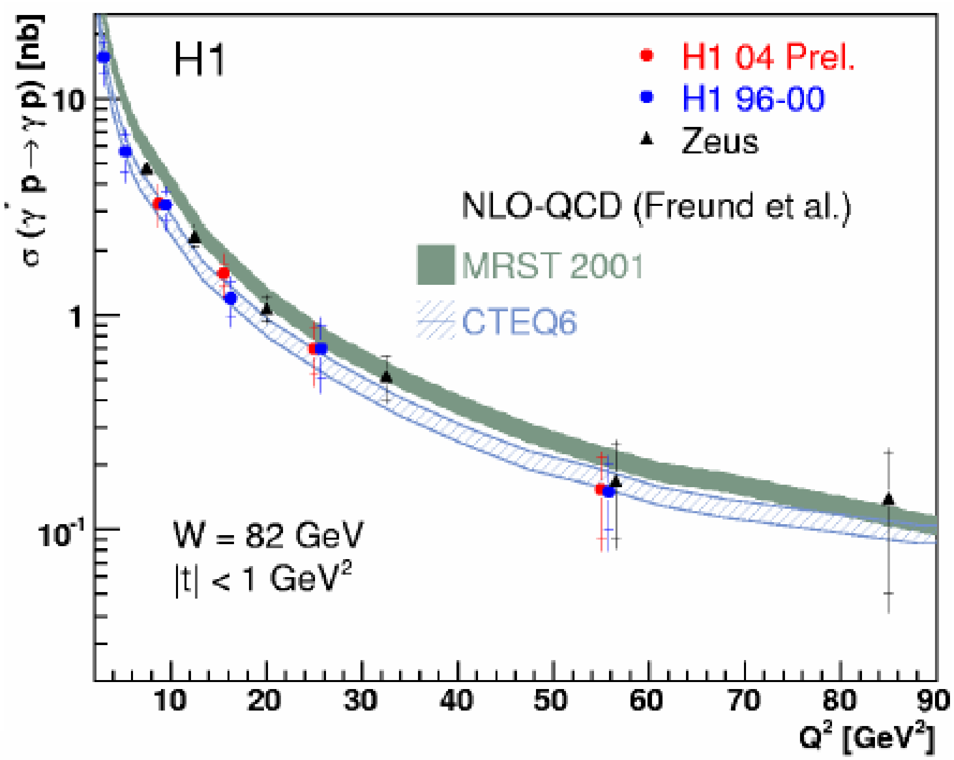

❖ **eRHIC measurements of cross section will provide significant constraints**

Podsumowanie

From Stone Age to Bronze Age…

- GPD analyses are starting to be data-driven!
  - DVCS (azimuthal asymmetries)
  - DVMP
  - Form factors and wide-angle processes
- Important to disentangle x, ξ and t dependence!
  - Experimental binning
  - Theoretical parameterizations
  - Improved lattice constraints (chiral extrapol.)
- Long-term goal: ("wish/suggestion" by W.D. Nowak)
  - Define standards → Database for GPDs
  - Perform global fits

Backup slides

HERMES

Beam spin and charge asymmetry

Beam Spin Asymmetry

$\overleftrightarrow{e} p \to e' p' \gamma$

[PRL87,2001]

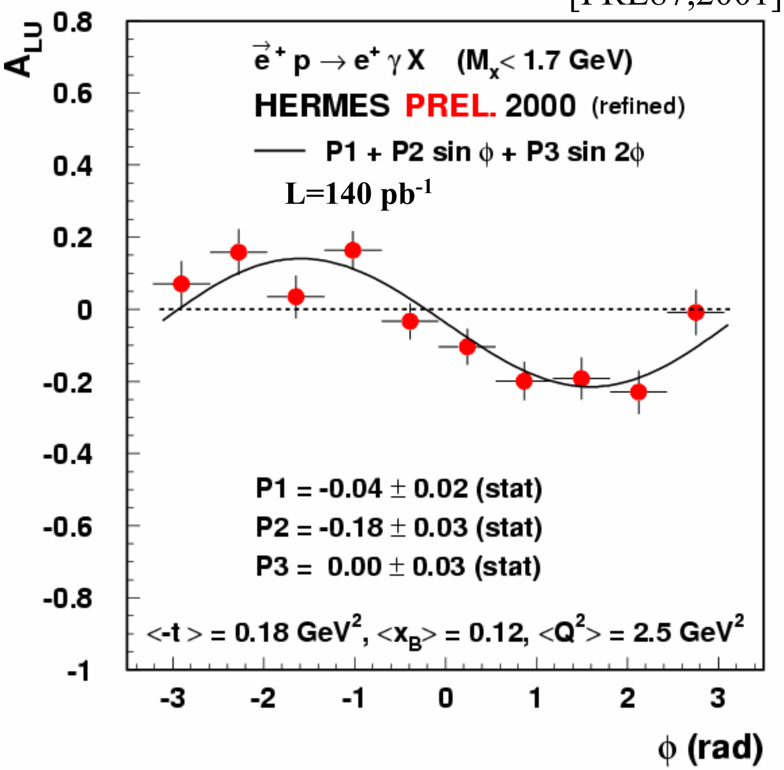

$$A_{LU} \propto \sin\phi \times \text{Im}(\tau_{BH}\tau_{DVCS})$$

Beam Charge Asymmetry

$e^{+/-} p \to e' p' \gamma$

symmetrization $\phi \to |\phi|$ (cancel sin ϕ terms from polarized beam)

[hep-ex/0605108, subm. to PRL]

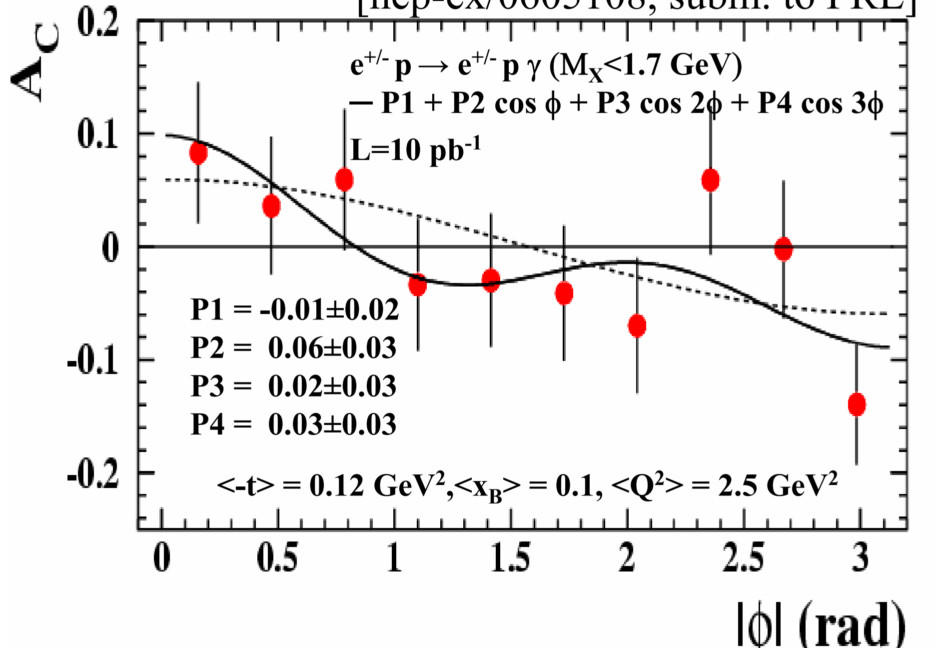

$$A_C \propto \cos\phi \,\text{Re}(\tau_{BH}\tau_{DVCS})$$

SIDIS Cross Section (up to subleading order in 1/Q)

$$d\sigma = d\sigma^0_{UU} + \cos 2\phi \, d\sigma^1_{UU} + \frac{1}{Q}\cos\phi \, d\sigma^2_{UU} + \lambda_e \frac{1}{Q}\sin\phi \, d\sigma^3_{LU}$$

$$+S_L \left\{ \sin 2\phi \, d\sigma^4_{UL} + \frac{1}{Q}\sin\phi \, d\sigma^5_{UL} + \lambda_e \left[d\sigma^6_{LL} + \frac{1}{Q}\cos\phi \, d\sigma^7_{LL} \right] \right\}$$

$$+S_T \left\{ \sin(\phi - \phi_S) \, d\sigma^8_{UT} + \sin(\phi + \phi_S) \, d\sigma^9_{UT} + \sin(3\phi - \phi_S) \, d\sigma^{10}_{UT} \right.$$

$$+ \frac{1}{Q}\left(\sin(2\phi - \phi_S) \, d\sigma^{11}_{UT} + \sin\phi_S \, d\sigma^{12}_{UT} \right)$$

$$\left. + \lambda_e \left[\cos(\phi - \phi_S) \, d\sigma^{13}_{LT} + \frac{1}{Q}\left(\cos\phi_S \, d\sigma^{14}_{LT} + \cos(2\phi - \phi_S) \, d\sigma^{15}_{LT} \right) \right] \right\}$$

σ_{XY}

Beam Target

Polarization

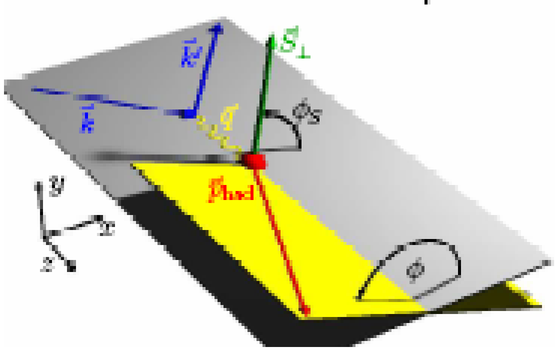

Mulders and Tangermann, Nucl. Phys. B 461 (1996) 197

Boer and Mulders, Phys. Rev. D 57 (1998) 5780

Bacchetta et al., Phys. Lett. B 595 (2004) 309

"Trento Conventions", Phys. Rev. D 70 (2004) 117504

Deep Exclusive experiments

Published ….. Preliminary results | 2004 | 2005 ……… ….. 2009 ? … | 2010

HERMES *27 GeV*	**HERA** *27.5-900 GeV*	**CLAS** *4-5 GeV*	**CLAS** *5.75 GeV*	**Hall A** *6 GeV*	**CLAS** *6 GeV*	**HERMES**	**COMPASS**	**JLab@** **12GeV**
DVCS – **BSA + BCA**	**DVCS**	**DVCS** **BSA**	**DVCS**	**DVCS** **proton** **neutron**	**DVCS** **Proton**	**DVCS** **BSA+BCA** *With recoil detector*	**DVCS** **σ+BCA** *With recoil detector*	EVERYTHING, **with more statistics** than ever before
+ nuclei **d-BSA** **d-BCA**			**DDVCS** **ΔDVCS** **D2VCS** **Polarized DVCS**					
$ep \to ep\rho$ σ_L + DSA								
			$ep \to ep\rho_L$	$ep \to ep\pi^o$	$ep \to ep\pi^o/\eta$			
$ep \to en\pi+$			$ep \to ep\omega_L$ $ep \to ep\pi^0/\eta$					
+ ….			$ep \to en\pi^+$ $ep \to ep\Phi$					

Kinematic Coverage of DVCS Experiments

Fixed-target experiments

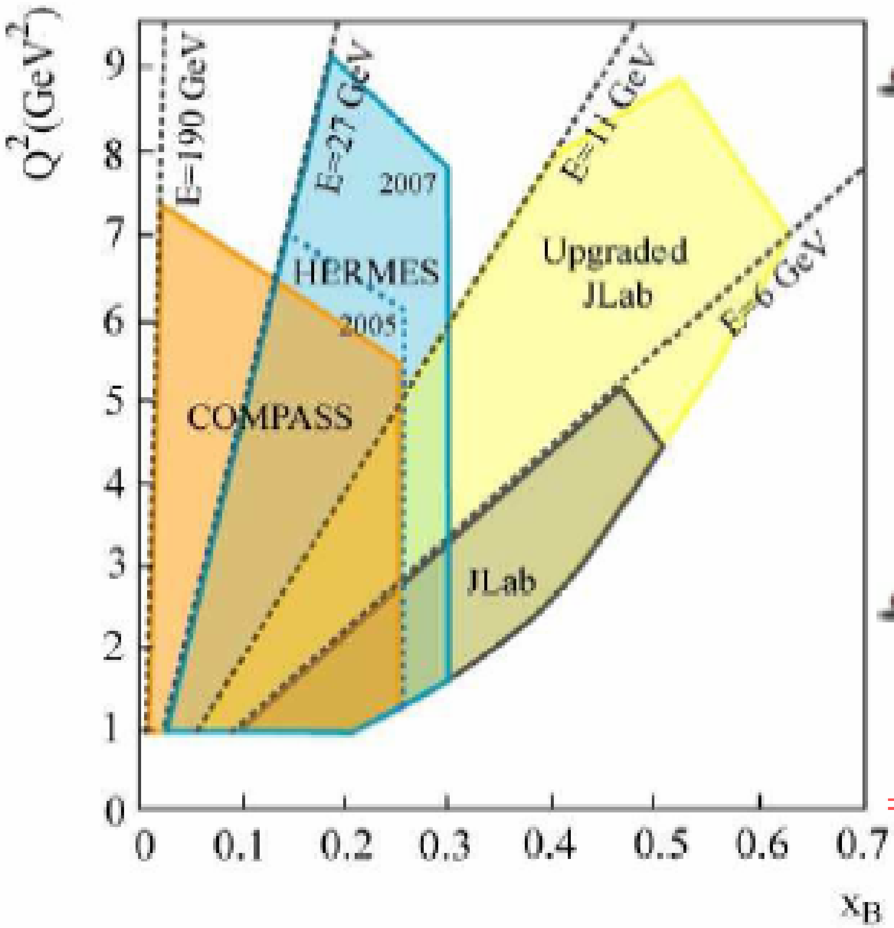

- Fixed-target experiments:

  $x > 0.03$, $Q^2 < 10$ GeV^2

  - COMPASS: low+medium x
  - HERMES: medium x, higher Q^2
  - JLab: medium+large x, lower Q^2
  - JLab 11 GeV: larger x, higher Q^2

- Collider experiments H1+ZEUS:

  $x < 0.01$, Q^2 : 5...100 GeV^2

$\Rightarrow$ almost no overlap